Ecotoxicology and Environmental Safety 152 (2018) 78–90

Contents lists available at ScienceDirect

Ecotoxicology and Environmental Safety

journal homepage: www.elsevier.com/locate/ecoenv

Toxicological effects of CdSe nanocrystals on the marine diatom *Phaeodactylum tricornutum*: The first mass spectrometry-based proteomic approach

Isabelle Poirier[a,b,*], Marie Pallud[a,c], Lauriane Kuhn[d], Philippe Hammann[d], Arnaud Demortière[e,f,g], Arash Jamali[e], Johana Chicher[d], Christelle Caplat[h], Régis Kevin Gallon[a,b], Martine Bertrand[a,b]

[a] *Institut National des Sciences et Techniques de la Mer, Conservatoire National des Arts et Métiers, 50103 Cherbourg en Cotentin Cedex, France*
[b] *Laboratoire Universitaire des Sciences Appliquées de Cherbourg, EA4253, Normandie Université, UNICAEN, 50130 Cherbourg en Cotentin, France*
[c] *IFREMER, LEAD NC, Equipe Ecophysiologie Station aquacole de Saint Vincent, Boulouparis, 98897 Nouvelle Calédonie Cedex, France*
[d] *Plateforme Protéomique Strasbourg Esplanade, CNRS FRC 1589, Institut de Biologie Moléculaire et Cellulaire, 67084 Strasbourg Cedex, France*
[e] *Laboratoire de Réactivité et Chimie des Solides, CNRS UMR 7314, Université de Picardie Jules Verne, 80039 Amiens Cedex 1, France*
[f] *Réseau sur le Stockage Electrochimique de l'Energie (RS2E), CNRS FR 3459, 80039 Amiens Cedex 1, France*
[g] *Center for Nanoscale Materials, Argonne National Laboratory, Argonne, IL 60439, United States*
[h] *UMR BOREA, UCBN, MNHN, UPMC, CNRS-7208, IRD-207, Institut de Biologie Fondamentale et Appliquée, Normandie Université, UNICAEN, 14032 Caen Cedex 5, France*

ARTICLE INFO

Keywords:
Marine microalgae
Nanoparticles
Toxicity
Physiological responses
Proteomics
Oxidative stress

ABSTRACT

In the marine environment, benthic diatoms from estuarine and coastal sediments are among the first targets of nanoparticle pollution whose potential toxicity on marine organisms is still largely unknown. It is therefore relevant to improve our knowledge of interactions between these new pollutants and microalgae, the key players in the control of marine resources. In this study, the response of *P. tricornutum* to CdSe nanocrystals (CdSe NPs) of 5 nm (NP5) and 12 nm (NP12) in diameter was evaluated through microscopic, physiological, biochemical and proteomic approaches. NP5 and NP12 affected cell growth but oxygen production was only slightly decreased by NP5 after 1-d incubation time. In our experimental conditions, a high CdSe NP dissolution was observed during the first day of culture, leading to Cd bioaccumulation and oxidative stress, particularly with NP12. However, after a 7-day incubation time, proteomic analysis highlighted that *P. tricornutum* responded to CdSe NP toxicity by regulating numerous proteins involved in protection against oxidative stress, cellular redox homeostasis, Ca^{2+} regulation and signalling, S-nitrosylation and S-glutathionylation processes and cell damage repair. These proteome changes allowed algae cells to regulate their intracellular ROS level in contaminated cultures. *P. tricornutum* was also capable to control its intracellular Cd concentration at a sufficiently low level to preserve its growth. To our knowledge, this is the first work allowing the identification of proteins differentially expressed by *P. tricornutum* subjected to NPs and thus the understanding of some molecular pathways involved in its cellular response to nanoparticles.

Significance: The microalgae play a key role in the control of marine resources. Moreover, they produce 50% of the atmospheric oxygen. CdSe NPs are extensively used in the industry of renewable energies and it is regrettably expected that these pollutants will sometime soon appear in the marine environment through surface runoff,

Abbreviations: NPs, nanoparticles; CdSe NPs, cadmium-selenium colloidal nanocrystals; NP5, cadmium-selenium colloidal nanocrystals of 5 nm in diameter; NP12, cadmium-selenium colloidal nanocrystals of 12 nm in diameter; QDs, quantum dots; TOPO, trioctylphosphine oxide; ODPA, octadecylphosphonic acid; TOP, trioctylphosphine; TEM, transmission electron microscopy; STEM, scanning transmission electron microscopy; HAADF-STEM, high angle annular dark field in scanning transmission electron microscopy; EDX-STEM, scanning transmission electron microscopy energy dispersive X-ray spectroscopy; ROS, reactive oxygen species; $[Cd]_{eq.}$, equivalent Cd concentration; $[Se]_{eq.}$, equivalent Se concentration; PAR, photosynthetically active radiation; AAS, atomic absorption spectrometry; DCF-DA, dichlorofluorescein diacetate; DCF, dichlorofluorescein; DDA, data-dependent acquisition mode; CID, collision-induced dissociation; nanoLC-MS/MS, nanoscale liquid chromatography coupled to tandem mass spectrometry; MS, mass spectrometry; AGC, automatic gain control; HCD, higher energy collisional dissociation; PSM, peptide spectrum matches; GLM, generalized linear model; FDR, false-discovery rate; XIC, extracted ion chromatograms; PCA, principle component analysis; EC50, median effective concentration; GPX, glutathione peroxidase; SeGPX, selenium-dependent glutathione peroxidase; PCD, programmed cell death; MASP, mucin-associated surface protein; SUMO, small ubiquitin-like modifier; TRD, tryptophan rich domain

* Corresponding author at: Institut National des Sciences et Techniques de la Mer, Conservatoire National des Arts et Métiers, 50103 Cherbourg en Cotentin Cedex, France.
E-mail addresses: isabelle.poirier@lecnam.net (I. Poirier), Marie.Pallud@ifremer.fr (M. Pallud), l.kuhn@ibmc-cnrs.unistra.fr (L. Kuhn), p.hammann@ibmc.u-strasbg.fr (P. Hammann), arnaud.demortiere@u-picardie.fr (A. Demortière), arash.jamali@u-picardie.fr (A. Jamali), j.chicher@ibmc-cnrs.unistra.fr (J. Chicher), christelle.caplat@unicaen.fr (C. Caplat), regis.gallon@lecnam.net (R.K. Gallon), martine.bertrand@lecnam.net (M. Bertrand).

https://doi.org/10.1016/j.ecoenv.2018.01.043
Received 8 November 2017; Received in revised form 17 January 2018; Accepted 19 January 2018
Available online 04 February 2018
0147-6513/

urban effluents and rivers. Since estuarine and coastal sediments concentrate pollutants, benthic microalgae which live in superficial sediments will be among the first targets of nanoparticle pollution. Thus, it is relevant to improve our knowledge of interactions between diatoms and nanoparticles. Proteomics is a powerful tool for understanding the molecular mechanisms triggered by nanoparticle exposure, and our study is the first one to use this tool to identify proteins differentially expressed by *P. tricornutum* subjected to CdSe nanocrystals. This work is fundamental to improve our knowledge about the defence mechanisms developed by algae cells to counteract damage caused by CdSe NPs.

1. Introduction

In the past two decades, research efforts have resulted in the gradual introduction of nanoparticles in numerous industrial fields, because of their unique optical, mechanical, electrical and magnetic properties (Stark et al., 2015). Nanoparticles containing a cadmium selenide core have recently attracted attention as promising photovoltaic devices (Hetsch et al., 2011) and their use in solar panel design is expanding (Wong et al., 2014). The cadmium selenide core is usually surrounded by a surface layer of organic and/or inorganic molecules named shell, but some environmental conditions can lead to a shell dissolution and a release of the CdSe core (Morelli et al., 2012). Toxicological effects of CdSe/ZnS quantum dots (QDs) on marine planktonic organisms have been the subject of several studies (Morelli et al., 2015; Scebba et al., 2016; Zhou et al., 2016), but the impact of the CdSe core alone has never been studied. The toxicity of uncoated metallic nanoparticles has been discussed in several reports and often deriving from dissolution of metal ions (Kirchner et al., 2005; Rzigalinski and Strobl, 2009; Baker et al., 2014). Previous studies have shown that the CdSe core dissolution is accelerated by its surface oxidation generated by aerobic conditions (Derfus et al., 2004; Zeng et al., 2015) or by light (Derfus et al., 2004). Moreover, Morelli et al. (2012) have shown that bare CdSe QDs, lacking the ZnS shell, underwent a salinity-dependent degradation process. Since CdSe nanocrystals are currently extensively used in the industry of renewable energies, it is regrettably expected that these new pollutants will sometime soon appear in the marine environment through surface runoff, urban effluents and rivers, and more particularly in estuarine and coastal sediments impacted by anthropogenic activities. Marine organisms living in estuarine and coastal sediments will be the first targets of these new pollutants. Among them, benthic microalgae play a key role in the control of marine resources and in global biogeochemical cycles; it is therefore relevant to improve knowledge about interactions between these microorganisms and nanoparticles. The diatom *P. tricornutum* appears as a good model to study these interactions for several reasons, (i) diatoms are the dominant microalgae in most marine ecosystems (Walsh, 1993), (ii) *P. tricornutum* has been completely sequenced (Bowler et al., 2008), (iii) this species has a high tolerance to cadmium (Brembu et al., 2011) and it was commonly used for assessing effects of nanoparticles in recent studies (CdSe/ZnS quantum dots: Morelli et al., 2015; Scebba et al., 2016; Zhou et al., 2016; TiO_2 NPs: Wang et al., 2016; Deng et al., 2017; Minetto et al., 2017; CeO_2 NPs: Deng et al., 2017; Sendra et al., 2017a; Ag NPs: Schiavo et al., 2017; Sendra et al., 2017b; CuNPs: Zhu et al., 2017 and ZnO NPs: Castro-Bugallo et al., 2014; Li et al., 2017). The authors focused on physiological and biochemical responses and highlighted the following major impacts: a growth inhibition (Zhou et al., 2016; Deng et al., 2017; Schiavo et al., 2017; Zhu et al., 2017), an increase in reactive oxygen species (ROS) production causing oxidative stress (Deng et al., 2017; Peng et al., 2017; Sendra et al., 2017a, b; Zhu et al., 2017), direct interactions between NPs and algae cells leading to membrane damages (Wang et al., 2016; Li et al., 2017; Schiavo et al., 2017; Sendra et al., 2017a, b), an increase in activity of antioxidant enzymes (Morelli et al., 2015; Wang et al., 2016; Deng et al., 2017) and a loss of photosynthetic pigments (Castro-Bugallo et al., 2014; Sendra et al., 2017b; Zhu et al., 2017). To our knowledge, only two previous studies used proteomics to analyse the impact of CdSe NPs on *P. tricornutum* (Morelli et al., 2015; Scebba et al., 2016). These studies have shown that CdSe/ZnS quantum dots can induce numerous proteome changes in *P. tricornutum*, but authors did not identify involved proteins. In our study, we have examined the response of *P. tricornutum* to CdSe nanocrystals through microscopic, physiological, biochemical and proteomic approaches. Proteins differentially expressed by algae cells submitted to NPs are identified by mass spectrometry analyses in order to elucidate strategies developed by this marine diatom to counteract the toxicity of NPs.

2. Materials and methods

2.1. Synthesis of CdSe colloidal nanocrystals

In previous studies, NPs with a diameter less than 30 nm were commonly used (Rocha et al., 2017). We have therefore chosen to test CdSe colloidal nanocrystals (CdSe NPs) with diameters of 5 nm and 12 nm (named NP5 and NP12, respectively, in the manuscript) (She et al., 2011, 2013). In addition, these two sizes would display different degrees of toxicity based on their volume and metal content (Morones et al., 2005; Monrás et al., 2014). CdSe NPs were synthesized in a 50 mL three-neck flask using a Schlenk-line approach. TOPO (3.0 g, Sigma-Aldrich-99%), ODPA (0.308 g, PCI Synthesis-97%), and CdO (0.060 g, Sigma-Aldrich-99%) were mixed, heated up to 150 °C, and kept under vacuum for 2 h. The reaction solution was then heated up to 300 °C under nitrogen at approximately 7 °C/min. Next, 1.5 g of TOP was rapidly injected into the reaction flask. TOP-Se solution (0.058 g Se, Aldrich-98% + 0.360 g TOP, Sigma-Aldrich, 90%) was then also injected of 360 °C and 330 °C for the synthesis of NP5 and NP12, respectively. For NP5, the reaction was quenched 60 s after the TOP-Se injection by the injection of 5 mL of room-temperature toluene. For NP12, the reaction solution was kept at high temperature for 180 s. After the solution cooled down to room temperature, the CdSe NPs were precipitated by adding ethanol and centrifuging; this washing step was repeated twice. Finally, the CdSe NPs were re-dissolved in toluene and stored inside a glove box under nitrogen atmosphere. The size measurement of the newly synthesized pristine nanoparticles was based on a transmission electron microscopy (TEM) image analysis using an automatic procedure (analyse particles) in the FIJI software. The study of their behaviour in aqueous solution, by TEM image analysis, highlighted a satisfactory stability (good dispersion and no meaningful change in size). The properties and characteristics of CdSe NPs are described in Supplementary Table 1.

2.2. Test species and culture conditions

The experiments were performed with the marine diatom *P. tricornutum* BOHLIN COUGHLAN/−632 axenic strain from the algal culture collection of the Göttingen University (SAG: Sammlung von Algenkulturen der Universität Göttingen), Germany. *P. tricornutum* was cultured in 250-mL flasks containing 100 mL of autoclaved f/2 medium realized with filtered natural seawater. Culture medium was inoculated at the cell density of about 8×10^5 cells/mL from a 7-day-old mother culture.

To determine the effect of CdSe NPs on growth, oxygen production, intracellular ROS level and proteome evolution of *P. tricornutum*,

culture medium was supplemented with NP5 to reach a concentration of 2.2×10^{14} NPs/L (83 µg/L; 0.37 nM), corresponding to an equivalent Cd concentration ($[Cd]_{eq.}$) of 47 µg/L (0.42 µM) and an equivalent Se concentration ($[Se]_{eq.}$) of 33 µg/L (0.42 µM), or with NP12 to reach a concentration of 4.2×10^{13} NPs/L (222 µg/L; 0.07 nM), corresponding to a $[Cd]_{eq.}$ of 127 µg/L (1.13 µM) and a $[Se]_{eq.}$ of 89 µg/L (1.13 µM). These concentrations are close to those predicted in estuarine and coastal sediments impacted by anthropogenic activities (expected between 1 µg/Kg and 10 mg/Kg; Gottschalk et al., 2013). Moreover, these concentrations provide similar exchange surface areas between NPs and diatoms ($1.8 \pm 0.1 \times 10^{16}$ nm^2/L) and therefore similar concentrations of surface metal atoms. Indeed, CdSe nanocrystal toxicity is mainly caused by the release of surface metal ions (Derfus et al., 2004) and some authors claim that the main source of toxicity of these particles is not their metal content but rather the interaction of the particle surface with the cells (Kirchner et al., 2005). Previously, a study realized by Kirchner et al. (2005) demonstrated the relevance of using the surface atom concentration instead of the particle concentration.

NP-supplemented and control cultures were grown at 20 °C, under a light-dark cycle (16 h/8 h, fluorescent tubes, 100 µmol photons/m^2/s PAR) for 12 days. They were manually stirred once a day.

The impact of lower and higher CdSe NP concentrations on growth was also studied ($[Cd]_{eq.}$ of 25, 600, 1200 and 2400 µg/L for NP5; $[Cd]_{eq.}$ of 50, 240, 460, 1200 and 2400 µg/L for NP12).

2.3. Dissolution of CdSe NPs in f/2 medium

NP dissolution in f/2 medium was evaluated over time by the quantification of the free Cd ions present in the supernatant after sedimentation of the undissolved NPs by ultracentrifugation. Erlenmeyer flasks containing 100 mL of f/2 medium were supplemented with NP5 or NP12 in order to reach the concentrations mentioned above. Two flasks (one for each size of NPs) were placed under a light-dark cycle (16 h/8 h, fluorescent tubes, 100 µmol photons/m^2/s PAR) and two flasks (one for each size of NPs) in the dark (to test the influence of the light on NP dissolution), at 20 °C for 7 days. All flasks were manually stirred once a day. At days 1, 4 and 7, 12 mL samples of all flasks were ultracentrifuged at 284,570 g during 4 h or 40 min for NP5 and NP12, respectively, to pellet the undissolved NPs. The time of centrifugation was calculated using the Stokes' law. The supernatants were recovered with care and used to quantify free Cd ions released from NPs by atomic absorption spectrometry (AAS) with an AAS 240FS instrument (Varian). The percentage of dissolution was calculated for each condition. All experiments were performed in triplicate.

In addition, two flasks supplemented with CdSe NPs (one for each size of NPs) were inoculated with diatoms (8×10^5 cells/mL), placed under a light-dark cycle (16 h/8 h, fluorescent tubes, 100 µmol photons/m^2/s PAR) at 20 °C and treated in the same way to study the ability of diatoms to immobilize the Cd ions released from NPs. For each size of NPs, the difference of Cd concentration of the supernatant between the two conditions (without and with diatoms) corresponds to the Cd ion concentration sequestered by diatoms. Sequestered Cd ions sediment with diatoms during ultracentrifugation, causing the decrease in the free Cd ion concentration of the supernatant, compared to the condition without diatoms. Knowing the cell concentration at each sampling time (determined by absorbance measurement at 600 nm), it is possible to calculate the mass of cadmium sequestered by diatom.

2.4. Growth kinetics

To determine the effect of NPs on the diatom growth, the growth kinetics of NP-supplemented and control cultures were followed simultaneously by a daily absorbance measurement at 600 nm using an Apollo-1 microplate reader (Berthold Technologies GmbG & Co. KG, Bad Wildbad, Germany). Absorbance values were converted into cell concentrations (diatoms/mL) using a calibration curve relating absorbance at 600 nm to cell concentration determined in a Malassez cell. After 12 days of culture, the growth rate was calculated for all culture conditions. All experiments were performed in triplicate.

2.5. Ability of P. tricornutum to sequester Cd ions released from NPs

The capacity of diatoms to immobilize Cd ions released from the complete NP dissolution was also estimated as described in a previous study (Poirier et al., 2014). Briefly, after 7 days of culture (time corresponding to the complete NP dissolution), 12 mL samples of NP-supplemented cultures were centrifuged (2 000 g; 10 min; 20 °C) after absorbance measurement at 600 nm to know cell density. The pellets were dried at 80 °C for 20 h and digested with 5 mL of 65% HNO_3 (Acros Organics). The digests were analysed by atomic absorption spectrometry with an AAS 240FS instrument (Varian). Results were expressed as µg Cd sequestered by cell. The experiment was performed in triplicate.

2.6. Preparation of samples for HAADF-STEM and EDX-STEM

HAADF-STEM (high angle annular dark field in scanning transmission electron microscopy) and EDX-STEM (scanning transmission electron microscopy energy dispersive X-ray spectroscopy) analyses were performed in order to observe the impacts of CdSe NPs and their released metal ions on *P. tricornutum*. After 7 days of culture, 20 mL samples of NP-supplemented and control cultures were filtered through a 0.45 µm sterile membrane (Sartorius France). Diatoms where collected from the membrane and re-suspended into natural seawater. Diatoms were then deposed onto holey carbon TEM grid (in contact with absorbance paper) by drop casting and dried using TEM pumping station for 15 min after being mounted in TEM specimen holder. FEI Tecnai G2-F20 STEM was used to analyse samples.

2.7. Oxygen production

After 2 and 7 days of culture, 10 mL samples of NP-supplemented and control cultures were centrifuged (2 000 g; 10 min; 20 °C) after absorbance measurement at 600 nm. The collected cells of *P. tricornutum* were washed twice with fresh f/2 medium. Finally, each pellet was re-suspended in fresh f/2 medium in order to get a diatom concentration of 3×10^6 cells/mL ($OD_{600\,nm} = 0.19$) just before analysis using a Clark-type oxygen electrode (Hansatech, King Lynn, UK). Each algal sample was kept in darkness during 15 min then irradiated by 500 µmol photon/m^2/s during 30 min in order to measure its O_2 production rate. All experiments were performed in triplicate.

2.8. Quantification of intracellular reactive oxygen species (ROS)

Intracellular ROS level in cells from NP-supplemented and control cultures was measured by following the cellular conversion of the non-fluorescent 2′,7′- dichlorofluorescein diacetate (DCF-DA) to the fluorescent compound dichlorofluorescein (DCF) as described by Wang and Joseph (1999), with minor modifications. After 1, 2, 3, 5 and 7 days of culture, 3 mL samples of NP-supplemented and control cultures were centrifuged (2 000 g; 10 min; 20 °C). The cells were re-suspended with a solution of 10 µM DCF-DA in sterile seawater (3 mL) by gentle agitation and left to react for 1 h, at room temperature in the dark. The reaction was stopped by centrifugation (2 000 g; 10 min; 20 °C) and re-suspending diatoms in sterile natural seawater (3 mL). Intracellular ROS level was quantified using an APOLLO-1 microplate reader (Berthold Technologies) by measuring fluorescence emission at 535 nm after excitation at 485 nm. Fluorescence emission intensity was normalized to cell density in the wells (diatoms/mL), determined itself by absorbance measurement at 600 nm. The results were expressed as a percentage of the control. All experiments were performed in triplicate.

2.9. Proteomics

2.9.1. Preparation of protein extracts

Protein extraction was performed as described previously (Poirier et al., 2008), with minor modifications. After 7 days, 100 mL samples of NP-supplemented and control cultures were filtered through a sterile cellulose nitrate membrane (0.45 µm pore diameter, Sartorius France). The collected diatoms were rinsed twice with a 0.6 M Tris buffer (pH 8.1), re-suspended with 15 mL of buffer and disrupted by three passages at 159 MPa through the pre-cooled French Press. The resulting homogenates were centrifuged for 1 h at 218,000 g at 4 °C with an OPTIMA L-100 XP ultracentrifuge (Beckman Coulter) to pellet down cell debris. The supernatants, containing extracted proteins, were purified, concentrated, freeze-dried and stored at − 20 °C until mass spectrometry analysis. For each culture condition (control, NP5 and NP12), protein extraction was performed in triplicate.

2.9.2. Mass spectrometry analyses

Protein extracts were quantified using a Bradford assay and prepared as described in a previous study (Poirier et al., 2016). Briefly, 10 µg of each sample were precipitated with 0.1 M ammonium acetate in 100% methanol and proteins were re-suspended in 50 mM ammonium bicarbonate. After a reduction-alkylation step (dithiothreitol 5 mM – iodoacetamide 10 mM), proteins were digested overnight with sequencing-grade porcine trypsin (1:25, w/w). Half of the resulting vacuum-dried peptides were re-suspended in 20 µL of water containing 0.1% (v/v) formic acid (solvent A).

The peptide mixtures were analysed by a first nanoscale liquid chromatography coupled to tandem mass spectrometry (nanoLC-MS/MS) using a NanoLC-2DPlus system (with nanoFlex ChiP module; Eksigent, ABSciex, Concord) coupled to a TripleTOF 5600 mass spectrometer (AB Sciex) operating in positive mode. Five microliters of each sample (1000 ng) were loaded on a ChIP C-18 precolumn (300 µm ID × 5 mm ChromXP; Eksigent) at 2 µL/min in solvent A. After 10 min of desalting and concentration, the pre-column was switched online with the analytical ChIP C18 analytical column (75 µm ID × 15 cm ChromXP; Eksigent) equilibrated in solvent A: solvent B (95:5; v/v). Solvent B composition was formic acid: acetonitrile (0.1:100; v/v). Peptides were eluted by using a 5–40% gradient of solvent B for 120 min at a flow rate of 300 nL/min. The TripleTOF 5600 was operated in data-dependent acquisition mode (DDA) with Analyst software (v1.6, AB Sciex). Survey mass spectrometry (MS) scans were acquired during 250 ms in the 350–1250 *m/z* range. Up to 20 of the most intense multiply charged ions (2 + to 5 +) were selected for collision-induced dissociation (CID) fragmentation, if they exceeded the 150 counts per second intensity threshold. Ions were fragmented using a rolling collision energy script within a 60 ms accumulation time and an exclusion time of 15 s. This so-called “Top20” method, with a constant cycle time of 1.5 s, was set in high-sensitivity mode.

The same samples were also submitted to a second nanoLC-MS/MS analysis on an Easy-nanoLC-1000 system coupled to a Q-Exactive Plus mass spectrometer (Thermo) operating in positive mode with a nanoelectrospray source. Five microliters of each sample (250 ng) were loaded on a C-18 precolumn (75 µm ID × 20 mm nanoViper, 3 µm Acclaim PepMap; Thermo) at 20 µL/min in solvent A. After desalting and concentration, the pre-column was switched online with the analytical C18 analytical column (75 µm ID × 25 cm nanoViper, 3 µm Acclaim PepMap; Thermo) equilibrated in solvent A: solvent B (95:5; v/v). Peptides were eluted at a flow rate of 300 nL/min using a gradient from 5% B to 20% B in 120 min, from 20% B to 32% B in 15 min, from 32% B to 95% B in 1 min and 95% B to 95% B during 24 min. The Q-Exactive Plus was operated in data-dependent acquisition mode (DDA) with Xcalibur software (Thermo). Survey MS scans were acquired at a resolution of 70 K at 200 *m/z* (mass range 350–1250), with a maximum injection time at 100 ms and an automatic gain control (AGC) set at 3e6. Up to 10 of the most intense multiply charged ions (≥ 2) were selected for a higher energy collisional dissociation (HCD) fragmentation with a normalized collision energy set at 27, at 17.5 K resolution, with a maximum injection time at 100 ms and AGC set at 1e3. A dynamic exclusion time of 20 s was applied during the peak selection process.

2.9.3. Mass spectrometry-based quantification: spectral count approach and statistical validation

MS datasets generated by the 2 mass spectrometers were searched against the complete proteome set from the *P. tricornutum* strain CCAP1055/1 UniProtKB database (release from 2016 to 08–22, organism ID = 556484, Proteome ID = UP000000759, 10465 sequences). The fasta sequences from human keratins and the porcine trypsin were added to the *P. tricornutum* sequences as well as their corresponding decoy entries (Database toolbox from MSDA, a proteomics software: https://msda.unistra.fr/). We used the Mascot algorithm (version 2.2, Matrix Science) to perform the database search with a decoy strategy. The resulting.dat Mascot files were then imported into Proline software (http://proline.profiproteomics.fr/) for further post-processing. Proteins were validated on Mascot pretty rank equal to 1% FDR on both peptide spectrum matches (PSM) and protein sets (based on score). Raw Spectral Count values were then imported into RStudio in addition to the MSnbase and msmsTests libraries. After normalization, a multidimensional plot allowed to visualise the variability between the replicates. The home-made R script was entirely based on the solution provided by the package EdgeR (https://bioconductor.org/packages/release/bioc/html/edgeR.html) which includes empirical Bayes methods to share information among features. The EdgeR GLM regression results were exported into a table using the xlsx library, and used to represent the log value from the adjusted p-value as a function of the log value from the fold change (Volcano plot graphic) using the plotly library.

2.9.4. Mass spectrometry-based quantification: MS1 label-free approach

The Paragon algorithm (ProteinPilot package, AB Sciex) was then used to perform a second database search on the same nanoLC-MS/MS dataset and with the same decoy *P. tricornutum* database. Proteins validated by Paragon at FDR 1% were submitted to a MS1 label-free quantification. For that purpose, only non-modified and unshared peptides were considered, as well as the Paragon identification confidence threshold set at 99%. Precursor ions fulfilling these criteria were transferred into PeakView package (v 2.0 with Protein Quantitation plug-in, AB Sciex) and their corresponding eXtracted Ion Chromatograms (XIC) were automatically integrated, using the following parameters: RT window ± 2 min, MS tolerance ± 0.05 Da. To normalize and further process the MS1 label-free data, MarkerView software (v 1.2, AB Sciex) was used: a correction factor was first applied to each condition according to the “Total Area Sum” function. The statistical module from MarkerView then allowed us to perform a Principle Component Analysis (PCA) and a Student t-test on the triplicate experiments from each of the 3 tested conditions (control, NP5 and NP12). Finally, two different tables were generated containing either the peptide areas or the protein areas: as for MS1 label-free quantification, we averaged the areas from triplicate injections and calculated the ratio by dividing the average area obtained in the presence of NPs by the average area obtained in the control condition. A manual reconstruction of the peptides elution peaks was performed in a second instance, using the same software (PeakView, AB Sciex), to check whether the automatic integration process was being properly applied. A new ratio between NP supplemented and control conditions was calculated using average areas obtained by the manual reconstruction.

Only proteins presenting a sample/control ratio (Fold change) ≥ 2 or ≤ 0.5 for the three analyses (spectral count quantification with the Q-Exactive Plus mass spectrometer, spectral count quantification with the TripleTOF 5600 mass spectrometer and MS1-Label-Free quantification with the TripleTOF 5600 mass spectrometer) were validated as

regulated by CdSe NPs.

2.10. Statistical analysis

Results were expressed as mean ± standard deviation of the triplicates. The Student *t*-test was used to know whether the mean values were significantly different depending on the various treatments at the $p \leq .05$ level. Statistical analysis was performed using R software version 3.2.0.

3. Results and discussion

3.1. Dissolution of CdSe NPs in f/2 medium

The dissolution of CdSe NPs in f/2 medium was followed over time by separating free Cd ions and undissolved NPs by ultracentrifugation. The results are presented in Fig. 1. When NP5 and NP12 were introduced in f/2 medium, their dissolution over time was observed for all conditions (under a light-dark cycle and in the dark). Under a light-dark cycle, the NP dissolution was complete after a 7-day incubation time, while it was partial in the dark (82% and 29% for NP5 and NP12, respectively). Thus, although CdSe NPs used in our study showed a satisfactory stability in aqueous solution, seawater salinity and light lead to their dissolution. These results are in accordance with the study of Morelli et al. (2012) which demonstrated that bare CdSe QDs, lacking the ZnS shell, exhibited a salinity-dependent propensity to degrade with a consequent release of bioavailable forms of Cd. A faster metal ion release from metallic NPs in seawater was also observed in recent studies (Ag from AgNPs: Sendra et al., 2017b; Cu from CuNPs: Zhu et al., 2017). Moreover, previous studies have shown that the CdSe core dissolution is enhanced by oxidation via air and light (Derfus et al., 2004; Zeng et al., 2015), two conditions being coupled in our experiments.

3.2. Effect of CdSe NPs on growth

The effects of CdSe NPs on the growth kinetics of *P. tricornutum* cultured in f/2 medium at 20 °C under a light-dark cycle (16 h/8 h) are presented in Supplementary Fig. 1, Supplementary Table 2 and Fig. 2. NP5 gradually decreased the growth rate of *P. tricornutum* in the range 25–2400 µg/L $[Cd]_{eq.}$, with a strong impact from 600 µg/L [Cd]eq. (EC50 concentration). NP12 gradually decreased the growth rate of *P. tricornutum* in the range 50–460 µg/L $[Cd]_{eq.}$ and the growth was completely inhibited from 1200 µg/L $[Cd]_{eq.}$ Several previous studies have reported the impact of nanoparticles on the growth rate of *P. tricornutum*. It was negatively affected by CdSe/ZnS QDs (Morelli et al., 2015; Scebba et al., 2016; Zhou et al., 2016), TiO_2 NPs (Wang et al., 2016; Deng et al., 2017; Minetto et al., 2017), CeO_2 NPs (Deng et al., 2017; Sendra et al., 2017a), ZnO (Castro-Bugallo et al., 2014; Li et al., 2017), Y2O3 (Castro-Bugallo et al., 2014) and AgNPs (Schiavo et al., 2017; Sendra et al., 2017b).

When *P. tricornutum* was exposed to NP5 and NP12 concentrations corresponding to a similar exchange surface between NPs and diatom cells (47 µg/L $[Cd]_{eq.}$ and 127 µg/L $[Cd]_{eq.}$ for NP5 and NP12, respectively; 33 µg/L $[Se]_{eq.}$ and 89 µg/L $[Se]_{eq.}$ for NP5 and NP12, respectively), stronger growth disorders were observed with NP12 (Fig. 2). Diatoms exhibited a high decrease in the growth rate (35%) and increase in the lag phase (4 days instead of 1 day for control and NP5). Previous studies have demonstrated that *P. tricornutum* is a highly tolerant species to cadmium toxicity and that a Cd concentration of several mg per liter medium is necessary to strongly impact its growth. For example, in the study of Torres et al. (2000) no significant growth rate inhibition was observed for Cd concentrations below 1 mg/L. In the same way, the growth rate of *P. tricornutum* was insignificantly reduced in cultures treated with 123 µg/L Cd during experiments carried out by Brembu et al. (2011). Thus, growth disorders observed in our study with NP12 should not be explained by their Cd level since the total NP12 dissolution releases only 127 µg Cd/L. Moreover, when NP5 and NP12 were used at the same $[Cd]_{eq.}$ concentrations (50 µg/L, 1200 µg/L and 2400 µg/L), a stronger negative impact on growth was observed with NP12 (Supplementary Fig. 1), showing that the toxicity of NP12 was not only induced by their Cd level. Depending on its concentration, selenium can act as an essential micro-nutrient protecting against reactive oxygen species damage or as a toxic compound. At low concentrations, it can be readily oxidized into the nontoxic Se° and converted into seleno-amino acids (selenocysteine and selenomethionine) which are incorporated in the structure of several antioxidant defence proteins (Kim et al., 2015). However, at high concentrations, it may become toxic by acting as pro-oxidant, primarily because of its capacity to replace sulfur (S) in proteins, which then lose their correct folding (Van Hoewyk et al., 2008). Concerning microalgae, several studies have shown that Se concentrations above 10 µM must be applied to impact the growth cell (for a review see Gojkovic et al., 2015); Se concentrations used in our study being below this value, Se alone cannot account for the negative impact of NP12 on *P. tricornutum* growth. Moreover, several studies have shown the protective effect of selenium in photosynthetic organisms exposed to cadmium (Saidi et al., 2014; Khan et al., 2015). The Cd-Se combination should therefore not be an aggravating factor. Nevertheless, it would be interesting, in further experiments, to test the impact of the combination of Cd and Se ions (127 µg/L and 89 µg/L, respectively) in order to clarify NP toxicity before they dissolve.

The negative impacts of NP12 on the diatom growth could be explained by direct physical interactions between NP12 and diatoms at the beginning of the cultures, before the total NP dissolution. Indeed, several previous studies have shown that metallic NPs interact with *P. tricornutum* cells by binding to the cell surface (Morelli et al., 2013; Deng et al., 2017; Minetto et al., 2017). In some cases, NPs can completely cover diatoms leading to cell wall damage (Wang et al., 2016; Sendra et al., 2017b) and cellular dysfunction because of the limitation of the nutrient intake (Deng et al., 2017). Moreover, a recent study has shown that CeO_2 NPs smaller than 20 nm can enter diatom cells (Sendra et al., 2017a). We can therefore assume that NPs used in our study

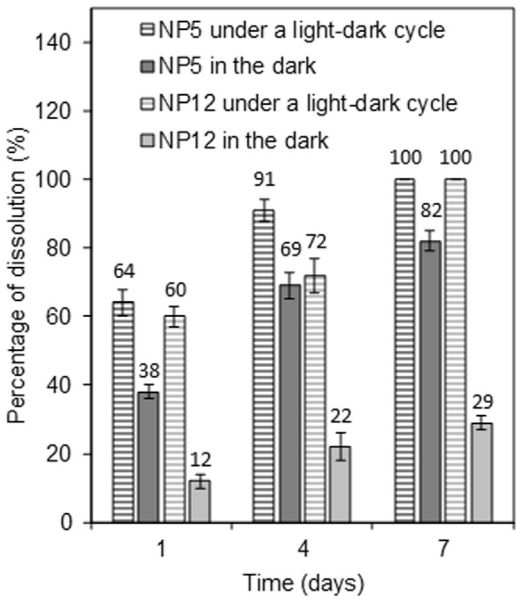

Fig. 1. Dissolution of NP5 (2.2×10^{14} NPs/L, $[Cd]_{eq.}$ = 47 µg/L, $[Se]_{eq.}$ = 33 µg/L) and NP12 (4.2×10^{13} NPs/L, $[Cd]_{eq.}$ = 127 µg/L, $[Se]_{eq.}$ = 89 µg/L) in f/2 medium, at 20 °C, under a light-dark cycle (16 h/8 h) or in the dark. The percentage of dissolved NPs was determined after 1, 4 and 7-d incubation times. Data are means ± standard deviations (n = 3). Some standard deviations are not visible because they are shorter than the symbol size.

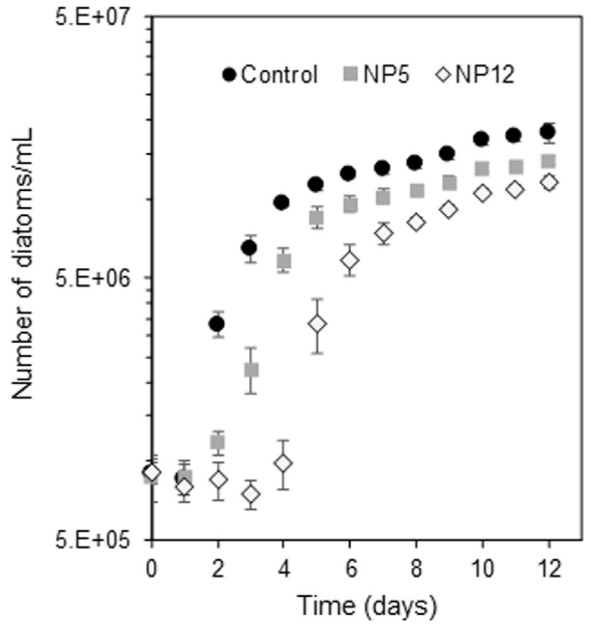

Fig. 2. Effect of CdSe NPs on the growth of *P. tricornutum*. The algae cells were cultured in f/2 medium, at 20 °C, under a light-dark cycle (16 h/8 h), without CdSe NPs (control), with NP5 (2.2×10^{14} NPs/L, $[Cd]_{eq.}$ = 47 µg/L, $[Se]_{eq.}$ = 33 µg/L) or with NP12 (4.2×10^{13} NPs/L, $[Cd]_{eq.}$ = 127 µg/L, $[Se]_{eq.}$ = 89 µg/L). Data are means ± standard deviations (n = 3). Some standard deviations are not visible because they are shorter than the symbol size.

could enter the cells leading to disturbances, such as an increase in ROS levels. Indeed, in a recent study, Xia et al. (2015) have demonstrated that elevated TiO_2 nanotoxicity in marine environments is related to increased ROS levels caused by the internalization of the TiO_2 NPs. In an additional study, direct physical interactions between CdSe NPs and diatoms and the NP internalization should be confirmed by HAADF-STEM analysis conducted before NP dissolution.

3.3. Interactions between diatoms and NPs

3.3.1. Capacity of P. tricornutum to sequester Cd released from CdSe NP

The presence of *P. tricornutum* in the NP-supplemented f/2 medium caused the decrease in free Cd concentration of the supernatant after ultracentrifugation, compared to the condition without diatoms (Supplementary Table 3). These results show the capacity of these diatoms to sequester a large part of the Cd ions released from NPs, leading them to sediment during ultracentrifugation. Based on these observations, we have calculated the amount of Cd immobilized by diatom for the three studied times, on the assumption that diatoms did not disturb the kinetics of NP dissolution (Supplementary Table 3). The results are presented in Fig. 3(a). With NP5, about 30×10^{-9} µg Cd was immobilized per diatom after 1 day of cultivation (cells in lag phase), while after 4 and 7-day incubation times, the amount of Cd sequestered per cell was 5×10^{-9} µg and 4×10^{-9} µg, respectively. With NP12, diatoms immobilized until 90×10^{-9} µg Cd per cell after a 1-day incubation time (cells in the lag phase), then this value decreased to reach 30×10^{-9} µg Cd per cell and 12×10^{-9} µg Cd per cell after 4-day (growth start) and 7-day incubation times, respectively. This decrease suggests an active Cd export, set up by diatoms to ensure their growth. An active Cd export by the diatom *P. tricornutum* was also suggested in a previous study (Brembu et al., 2011). Concerning undissolved NPs, our experiments did not allow us to say if they were immobilized by diatoms or not since the ultracentrifugation has led to their sedimentation in any case.

Moreover, after 7 days of cultivation, the Cd quantification in diatom cells by AAS confirmed that a large part of the Cd released from NPs was immobilized by diatoms (Fig. 3(b)). Diatoms cultured with NP5 contain 5×10^{-9} µg Cd/cell, which represents the Cd level of 24×10^{3} NP5. Diatoms cultured with NP12 contain 15×10^{-9} µg Cd/cell, which represents the Cd level of 5×10^{3} NP12 (Fig. 3(b)). Therefore, in our experimental conditions, the NP5 and NP12 were totally dissolved after 7 days of cultivation and 90% ± 2% and 78% ± 8% of the Cd released by NP5 and NP12, respectively, was sequestered by diatoms. These results are in accordance with previous studies showing the biosorption capacity of the diatom *P. tricornutum*

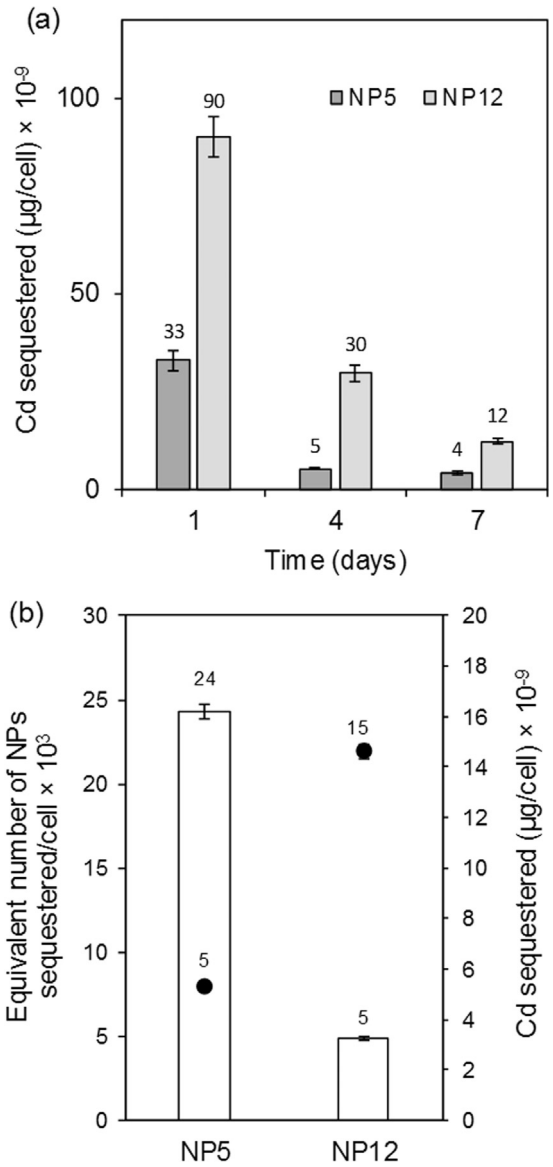

Fig. 3. Ability of *P. tricornutum* to sequester Cd ions released from CdSe NPs. (a): The masses of Cd sequestered by diatoms were determined by the quantification of free Cd ions present in the supernatant after sedimentation of the undissolved NPs and diatoms (when they are present) by ultracentrifugation (see Supplementary Table 3). f/2 medium supplemented with NP5 (2.2×10^{14} NPs/L, $[Cd]_{eq.}$ = 47 µg/L, $[Se]_{eq.}$ = 33 µg/L) or with NP12 (4.2×10^{13} NPs/L, $[Cd]_{eq.}$ = 127 µg/L, $[Se]_{eq.}$ = 89 µg/L) and inoculated with diatoms or not, was incubated at 20 °C, under a light-dark cycle (16 h/8 h). The measurements were realized after 1, 4 and 7-d incubation times. Data are means ± standard deviations (n = 3). (b): Cd ions (black circles) and equivalent number of CdSe NPs (bars) sequestered by *P. tricornutum*. The masses of Cd sequestered by diatoms were determined by the quantification of Cd ions from digested diatoms after 7 days of culture. The algal cells were cultured in f/2 medium supplemented with NP5 (2.2×10^{14} NPs/L, $[Cd]_{eq.}$ = 47 µg/L, $[Se]_{eq.}$ = 33 µg/L) or with NP12 (4.2×10^{13} NPs/L, $[Cd]_{eq.}$ = 127 µg/L, $[Se]_{eq.}$ = 89 µg/L), at 20 °C, under a light-dark cycle (16 h/8 h). Data are means ± standard deviations (n = 3).

for Cd ions. Indeed, Torres et al. (2014) have shown that this species could accumulate until 67 mg Cd/g and Brembu et al. (2011) until 13 × 10^{-12} mg Cd/cell. Moreover, when this species was exposed to bare CdSe quantum dots, lacking shell, the bare dissolution was followed by a Cd bio-accumulation at a similar rate as cells exposed to $CdCl_2$ (Morelli et al., 2012).

3.3.2. Microscopic observations

Microscopic observation of *P. tricornutum* cells cultured with CdSe NPs are presented in Fig. 4, Supplementary Fig. 2 and Supplementary Fig. 3. Microscopic observations were realized from 7-d old cultures. No significant morphology changes were observed for cells cultured in f/2 medium contaminated with NP5 (Supplementary Fig. 2(b)), except perhaps an increase in the number of ovoid cells. On the other hand, some diatom cells (about 20%) cultured in f/2 medium contaminated with NP12 presented modifications of the cell shape (Supplementary Fig. 2(c)). Alterations of cell shape were also observed in previous studies when *P. tricornutum* was treated with TiO_2 and CeO_2 NPs (Deng et al., 2017) and when *Tetraselmis suecica* was submitted to Ag NPs (Schiavo et al., 2017). HAADF-STEM and EDX analysis highlighted a high Se and Cd accumulation inside the cell wall (Supplementary Fig. 3), especially in the extreme parts (Fig. 4(c), (f), (g)), confirming the ability of *P. tricornutum* to immobilize metal ions released from CdSe NPs. The wall of this diatom is composed of silica and organic matter, including proteins, long chain polyamines and polysaccharides. The main polysaccharide is a sulphated glucuronomannan (Le Costaouëc et al., 2017) and a previous study has demonstrated the high capability of sulphated polysaccharides to sequester metal ions (Raize et al., 2004). HAADF-STEM analysis confirmed that diatoms cultured with NP12 presented cell shape modifications (Fig. 4(b)) and cell wall alterations (Fig. 4(c)) including breaks and a decrease in its thickness making it possible the visualization inside the cell, unlike the control (Fig. 4(a)). The capacity of NPs to induce cell wall damage was also observed in previous studies (Wang et al., 2016; Sendra et al., 2017a, b). HAADF-STEM analysis highlighted the presence of dense areas inside the cytosol corresponding probably to a vacuole (Fig. 4(d)) and lipid vesicles and/or stress granules (Fig. 4(e)). The vacuole is a multifunctional compartment central to many functions such as storage, catabolism and maintenance of the homeostasis (Shebanova et al., 2017). Several previous studies have shown its capacity to accumulate phosphorus and nitrogen reserves under stress conditions (Shebanova et al., 2017) and to sequester various pollutants including Cd (Brembu

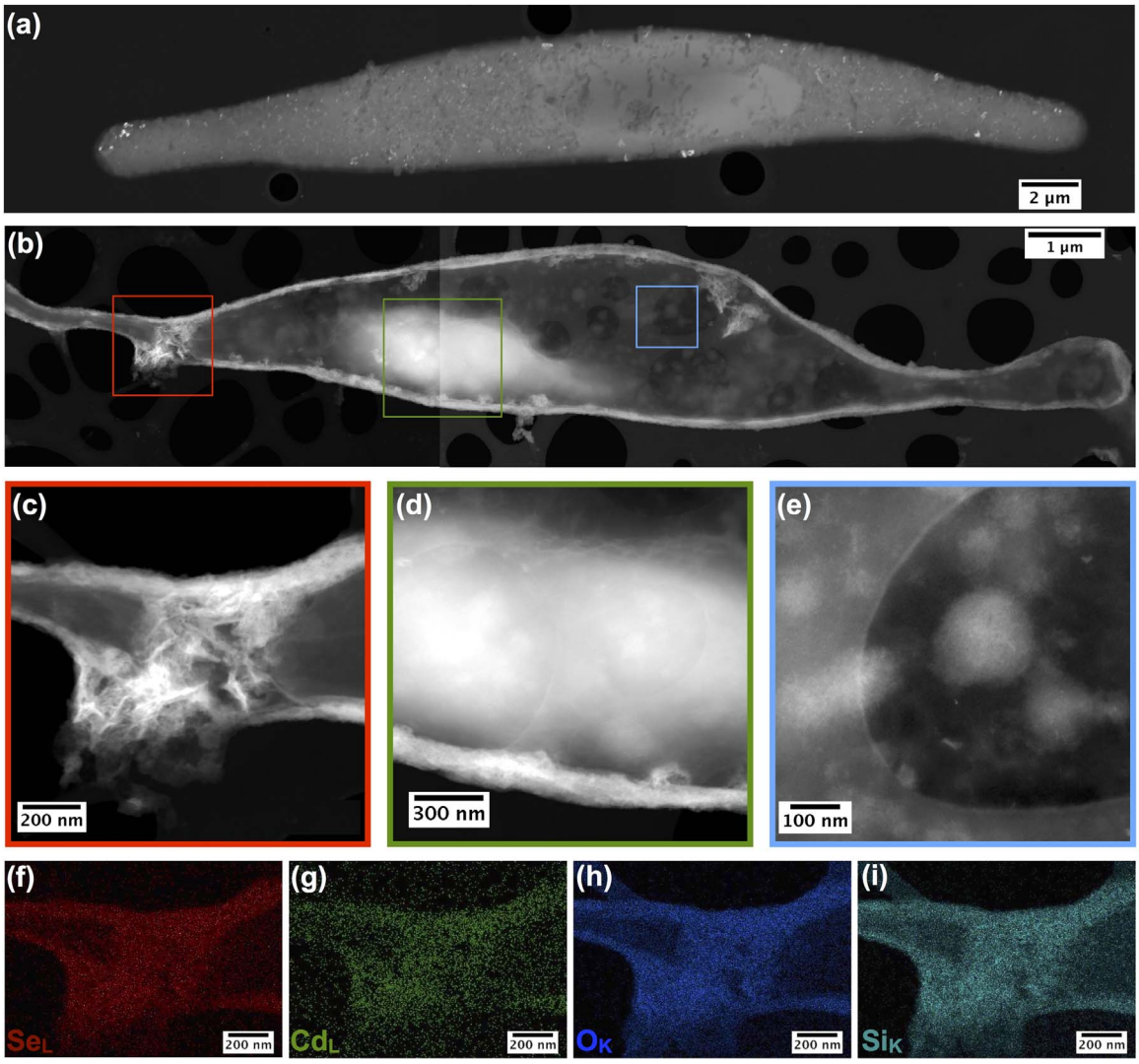

Fig. 4. HAADF-STEM analysis of *P. tricornutum*. Analysis were performed from 7-d-old cultures (a): HAADF-STEM image of a diatom cultured in f/2 medium without CdSe NPs (control). A regular shape is observed as well as a thick cell wall making it difficult to visualise inside the cell. (b) HAADF-STEM image of a diatom cultured in f/2 medium contaminated with NP12 (4.2×10^{13} NPs/L, $[Cd]_{eq.}$ = 127 µg/L, $[Se]_{eq.}$ = 89 µg/L). The cell exhibits cell shape modifications, especially in the extreme parts, and cell wall alterations including a decrease in the thickness of the cell wall making it possible to visualise inside the cell. (c): Dense and altered area of the cell wall. (d): Dense area of the cytosol corresponding probably to a vacuole. (e): Granules inside the cell. (f-i): EDX analysis reveals the presence of Se and Cd elements inside the cell wall.

et al., 2011). Indeed, in a previous study, Brembu et al. (2011) mentioned a possible Cd sequestration in the vacuole of *P. tricornutum* thanks to a vacuolar iron transporter homologue. This storage activity could explain its high density evidenced by HAADF-STEM analysis. The accumulation of lipid vesicles in microalgae under stress was demonstrated in a previous study (Elsayed et al., 2017) and it is known that lipid vesicles can be used by microorganisms to store pollutants (Verdin et al., 2005). So, we can hypothesise that *P. tricornutum* has probably internalised a part of Cd and Se released from CdSe NPs inside vacuole and lipid vesicles. However, although the presence of Se appears to be stronger in the vacuole (EDX analysis presented in Supplementary Fig. 3), the distribution of Cd and Se are homogeneous within the cells and it is difficult to draw conclusions. The internalization of Cd and Se in the vacuole and lipid vesicles should be confirmed by further experiments.

Stress granules are non-membranous cytoplasmic foci composed of non-translating messenger ribonucleoproteins that rapidly aggregate in cells exposed to adverse environmental stress conditions including oxidative stress (Anderson and Kedersha, 2009). They contain transcripts encoding housekeeping genes but exclude those encoding stress-induced genes which must be primarily translated. They range in size from 100 nm to 1000 nm (Anderson and Kedersha, 2009) which corresponds to the size of granules detected in diatoms cultured with NP12. Moreover, NPs can induce the stress granule formation (Santimano et al., 2013).

3.4. Effect of CdSe NPs on oxygen production

The impact of CdSe NPs on the oxygen production of *P. tricornutum* is presented in Supplementary Fig. 4. After 2 d of cultivation, a slight decrease in oxygen production (10%) was observed with NP5 (cells in exponential growth phase as for the control) (p-value = .036), while the oxygen production under NP12 stress (cells always in lag phase) was like control. After 7 days of culture (NP5 and control: cells at the beginning of the stationary growth phase; NP12: cells at the end of the exponential growth phase) a similar oxygen production was found for all conditions. Moreover, it should be noted a significant reduction of oxygen production between 2-d and 7-d incubation times for all culture conditions (− 35% for control, − 33% for NP5 and − 35% for NP12). As a result, in our experimental conditions, CdSe NPs did not strongly impact oxygen production. Our strain achieved to maintain a satisfactory O_2 production and so a satisfactory photosynthesis activity and energy production. This ability probably helps the cells to develop resistance mechanisms to counteract disturbances generated by NPs and released metal ions. In other studies, a decrease in photosynthetic activity is generally observed under NPs stress (Lin et al., 2009; Da Costa et al., 2016; Zhu et al., 2017).

3.5. Effect of CdSe NPs on intracellular ROS level

The intracellular ROS levels of *P. tricornutum* subjected to CdSe NPs are represented in terms of their relative increases (%) compared to the control (Fig. 5). In our experimental conditions, NP5 caused a significant increase in the intracellular ROS level only at day 5 of culture (2.7-fold; cells at the end of the exponential growth phase). Under NP12 exposure, a significant increase in the intracellular ROS level was observed at day 1 (5.7-fold; cells at the beginning of the lag growth phase), day 5 (7.9-fold; cells in exponential growth phase) and day 7 (4.0-fold; cells at the end of the exponential growth phase). The high intracellular ROS level observed in diatoms cultured with NP12 after 1 day of culture can be correlated to the high Cd accumulation level observed for the same time (Fig. 3(a)). Indeed, the major NP dissolution observed after one day of culture (60% of NP5 and 64% of NP12) led to a higher release of metal ions with NP12 than with NP5 (three times higher). Moreover, these results support also the hypothesis of direct physical interactions between CdSe NPs and cells (adsorption around the cells and internalization), before NP dissolution, leading to membrane damages as it was demonstrated in several previous studies (Wang et al., 2016; Sendra et al., 2017b; Schiavo et al., 2017). We can assume that NP12 caused more damage and ROS generation than NP5, because of their higher volume. Direct interactions between NPs and algae cells are reported to induce oxidative stress (Deng et al., 2017; Sendra et al., 2017b), which has been considered as the dominant factor in determining NP toxicity to microalgae (Xia et al., 2015; Peng et al., 2017). An increase in ROS level under NP stress was frequently observed in previous studies (Wang et al., 2016; Sendra et al., 2017a, b; Zhu et al., 2017). In an additional study, direct physical interactions between CdSe NPs and diatoms should be confirmed by HAADF-STEM analysis conducted before NP dissolution.

The lack of increase in intracellular ROS level with NP5 at 1, 2 and 3-d incubation times, and the strong decrease in intracellular ROS level under NP12 exposure between days 1 and 2, show the powerful antioxidant capacity of this diatom. *P. tricornutum* was capable to counteract effectively and rapidly the oxidative stress generated by CdSe NPs, probably thanks to metabolic changes which will be highlighted by our proteomic analysis. Comparable results were observed in recent studies (Wang et al., 2016; Sendra et al., 2017a; Zhu et al., 2017). During the exponential phase, which is a growth phase generating important ROS production because of a higher metabolic activity, cells cultured with NPs presented some difficulty to maintain low ROS levels and an increase in intracellular ROS level was observed at day 5. However, after 7 days of cultivation (cells at the beginning of the stationary phase with NP5 and at the end of the exponential growth phase with NP12) cells managed, once again, to decrease the ROS level, probably thanks to complementary metabolic adaptations. Changes in intracellular ROS levels during the different growth phases were also

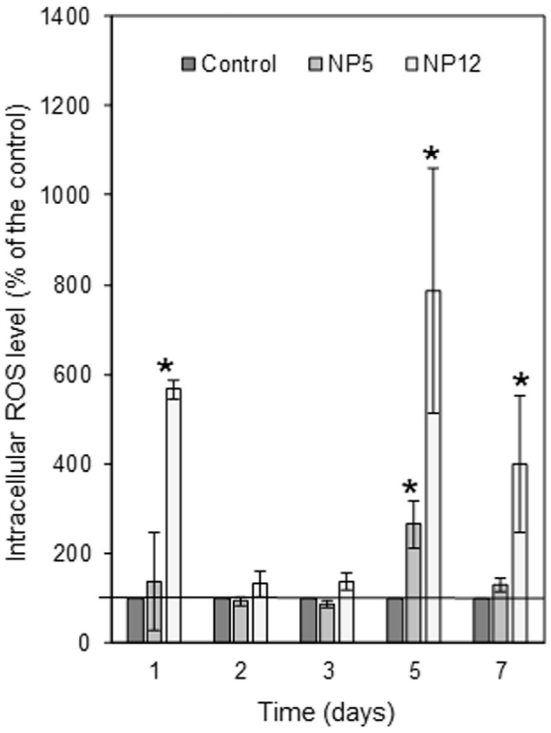

Fig. 5. Effect of CdSe NPs on intracellular ROS level in *P. tricornutum*. The algae cells were cultured in f/2 medium, at 20 °C, under a light-dark cycle (16 h/8 h), without CdSe NPs (control), with NP5 (2.2×10^{14} NPs/L, $[Cd]_{eq.}$ = 47 µg/L, $[Se]_{eq.}$ = 33 µg/L) or with NP12 (4.2×10^{13} NPs/L, $[Cd]_{eq.}$ = 127 µg/L, $[Se]_{eq.}$ = 89 µg/L). The measurements were performed from 1, 2, 3, 5 and 7-d-old cultures. The results were expressed as a percentage of the control (control value corresponding to the 100%). Data are means ± standard deviations (n = 3). Some standard deviations are not visible because they are shorter than the symbol size. The mean value of each bar with an asterisk (*) is significantly different from control according to Student t-test ($p \leq .05$).

observed in a previous study when *P. tricornutum* was subjected to AgNPs (Sendra et al., 2017b).

3.6. Differential protein expression

Only proteins presenting a sample/control ratio (fold change) ≥ 2 or ≤ 0.5 for the three quantification strategies (spectral count quantification with Q-Exactive+, spectral count quantification with TT5600 and MS1-Label-Free quantification with TT5600) were considered as regulated by CdSe NPs. The NP5 induced the up-regulation of 20 proteins and the down-regulation of 6 proteins (Supplementary Table 4), while NP12 induced the up-regulation of 28 proteins and the down-regulation of 7 proteins (Supplementary Table 5).

Eighteen differentially regulated proteins were common to both sizes of CdSe NPs (proteins on a grey background in Supplementary Tables 4 and 5). Identified proteins were found to be involved in various biological activities, such as oxidation-reduction process (e.g., alcohol dehydrogenase, thioredoxin), glycolytic process/energy metabolism (e.g., cytosolic aldolase, phosphoglycerate kinase), transport and binding (e.g., annexins, nucleic acid binding proteins for NP5), response to oxidative stress (e.g., actin binding protein, glutathione peroxidase for NP5, protein implied in thiamine biosynthesis for NP12), translation (e.g., structural constituents of ribosomes), protein metabolism (e.g., metallopeptidase for NP12), membrane biogenesis (e.g., integral components of membrane, phosphoric diester hydrolase for NP12), regulation/signalling (e.g., small ubiquitin-like modifier for NP12), energy metabolism (adenylate kinase for NP5) and other functions (e.g., metacaspase, TRD3).

In the following, we discuss the implications of these proteome changes in order to better understand impacts of CdSe NPs on algae cells and elucidate defence mechanisms developed by *P. tricornutum* to counteract damage induced by these NPs.

3.6.1. The fight against oxidative stress

The proteome analysis of *P. tricornutum* submitted to CdSe NPs has highlighted numerous metabolic changes to fight against oxidative stress. Thus, our results have shown the up-regulation of several proteins implied in oxidation-reduction processes and antioxidative activities such as alcohol dehydrogenase (NP5; NP12), thioredoxin (NP5; NP12), glutathione peroxidase (NP5) and protein implied in thiamine biosynthetic process (NP12). Alcohol dehydrogenase was also induced in *Cyanobacterium* PCC 6803 upon exposure to salt or hyperosmotic stress (Vidal et al., 2009) and the authors suggested a possible role for this enzyme in oxidizing NADPH under some stress conditions and thus contributing to the maintenance of the ATP/NADPH balance. It was also overexpressed in *Arabidopsis* NRAMP1 under Fe-deficiency (Vatansever et al., 2016). Thioredoxin is a small multifunctional protein involved in redox regulation (Marchand et al., 2006). Thioredoxin system is a key system against oxidative stress through its disulfite reductase activity regulating protein dithiol/disulphide balance (Lu and Holmgren, 2014). The up-regulation of the cytosolic aldolase and a protein implied in actin filament depolymerisation highlighted that *P. tricornutum* used S-nitrosylation and S-glutathionylation processes to decrease oxidative stress and maintain redox homeostasis. Indeed, cytosolic aldolase was identified as a potential target of S-nitrosylation and S-glutathionylation for thioredoxin (Marchand et al., 2006). Moreover, the depolymerisation of the actin filament could promote its S-glutathionylation and consequently could attenuate the effect of Cd ions released from NPs (Dailianis et al., 2009). Dailianis et al. (2009) suggested that the actin polymerization/depolymerisation regulation is involved in Cd-induced toxicological cell signalling responses. The S-glutathionylation of actin, which is considered as an early mechanism of protection against stress (Shelton et al., 2005), was also observed in a previous study in response to oxidative stress (Go et al., 2013). Glutathione peroxidase (GPX) is a powerful antioxidant agent able to scavenge H_2O_2 and to reduce lipid hydroperoxides (Cabello-Hurtado et al., 2016). An induction of this enzyme was also observed in *Arabidopsis thaliana* cells submitted to silica NPs (Cabello-Hurtado et al., 2016), in *Chlamydomonas reinhardtii* under vital consequences of copper stress (Jiang et al., 2016) and in the green microalgae *Ankistrodesmus falcatus* under nickel stress (Martínez-Ruiz and Martínez-Jerónimo, 2015). The high induction of the GPX indicates that NP5 have led to a ROS production, as it was demonstrated by our results presented Fig. 5, but defence mechanisms developed by *P. tricornutum* allowed to maintain ROS levels like control after one day of culture. GPXs are divided into two sub-families including selenium-dependent glutathione peroxidase (SeGPX) and non-selenium glutathione peroxidase (non-SeGPX). Previous studies have reported the expression of a SeGPX in marine organisms such as the mussel *Mytilus galloprovincialis* (Chatziargyriou and Dailianis, 2010) or the abalone *Haliotis discus discus* (Bathige et al., 2015). While no study mentions this for *P. tricornutum*, the up-regulation of the GPX observed in our study suggests that the diatom used Se released from CdSe NPs to preferentially synthesize SeGPX.

Thiamine (vitamin b1) has a documented antioxidant activity in both plants and animals (Tunc-Ozdemir et al., 2009) and it may partly act to scavenge superoxide ions directly (Jung and Kim, 2003). The thiamine content of phytoplankton cells is affected by abiotic stress (Sylvander et al., 2013). In a recent study, authors have demonstrated that thiamine was capable to decrease oxidative stress generated by H_2O_2 in the yeast *Saccharomyces cerevisiae* (Wolak et al., 2014). Thus, the over-synthesis of thiamine under NP12 stress helped *P. tricornutum* to fight against oxidative stress by contributing to a decrease in ROS level during cultivation.

In our study, the oxidative stress generated by CdSe NPs was also confirmed by the up-regulation of annexins. Annexins are multi-functional membrane-binding proteins that are involved in various stress responses and that can form Ca^{2+} permeable conductance in an oxidized membrane, simulating ROS signalling conditions (Laohavisit et al., 2010). Consequently, the over-expression of annexins led to an increase in intracellular Ca^{2+} level and the trigger of defence mechanisms against oxidative stress, as it was demonstrated in a previous recent study (Zhang et al., 2017). The increase in intracellular Ca^{2+} level probably led to a Ca^{2+} uptake into the vacuole, contributing to its high density highlighted by HAADF-STEM analysis. The vacuole is a major calcium store in many organisms and the removal of Ca^{2+} from the cytosol is essential to cellular Ca^{2+} homeostasis (for a review see Pittman, 2011).

In our culture conditions, metabolic changes described above have allowed *P. tricornutum* to maintain low ROS level after two and three-day incubation times (Fig. 5). However, after a 5-day culture period, these defence mechanisms became insufficient and an increase in ROS level was observed for contaminated cultures. This increase could explain the over-expression of the metacaspase highlighted by proteomic analysis. Metacaspases are cysteine proteases capable to mediate programmed cell death (PCD) in response to ROS (Fagundes et al., 2015; Bidle, 2016). The up-regulation of a metacaspase could explain the decrease in the specific growth rate observed with CdSe NPs (Supplementary Table 2) and suggest a regulation of the cell concentration, probably to provide extending population life. Previous studies have demonstrated that abiotic stress can trigger PCD, as well as an increase in antioxidant enzymes (González-Pleiter et al., 2017; Wang et al., 2017).

3.6.2. Other mechanisms developed to counteract stress generated by CdSe NPs

In our study, stress generated by CdSe NPs on *P. tricornutum* was also confirmed by the up-regulation of the phosphoglycerate kinase. Protein kinases play a significant role in cellular response to external stresses and stimuli since they are involved in metabolic adaptation during environmental stresses (Vercruysse et al., 2011). A protein kinase was also up-regulated in chickpea by TiO_2 NPs (Amini et al.,

2017). Moreover, phosphoglycerate kinase playing a key role for ATP production during glycolysis, the up-regulation of this enzyme indicates an increase in the energy demand of algae cells under CdSe NPs, probably to repair damage caused by NPs and maintain photosynthesis and growth. An over-expression of this protein under Cr stress was reported in a previous study (Bukhari et al., 2016), whereas its synthesis was down-regulated when the microalga *Microcystis aeruginosa* was submitted to AgNPs (Qian et al., 2016).

Our results show that CdSe NPs induced modifications in membrane composition of *P. tricornutum* since some of its components were up-regulated while other were down-regulated. With NP5, the down-regulation of a mucin-associated surface protein (MASP) was observed. MASPs are glycosylphosphatidylinositol-anchored glycoproteins and several studies have shown that sugar groups of glycoproteins can bind metal ions and NPs (Macfie and Welbourn, 2000; Deng et al., 2009). Sequestration of NPs and metal ions by membrane glycoproteins can protect cells by avoiding their penetration into cytosol. However, by interacting with the membrane, NPs and metal ions can induce impairment of its structure and function such as lipid peroxidation (Morelli et al., 2013; Tang et al., 2015). Consequently, our results show that *P. tricornutum* responded to stress generated by NPs and metal ions by reducing the level of membrane components facilitating direct interactions between the pollutants and the membrane in order to preserve membrane functionality.

With NP12, our results show the up-regulation of a protein implied in lipid metabolic process. Since lipid peroxidation is caused by an excess of ROS, the high ROS level observed with NP12 after one and five days of culture suggests a higher lipid peroxidation with NP12 than with NP5. As a result, in the presence of NP12, the algae cells must produce a high amount of lipids to replace those altered and ensure their growth. Several previous studies have shown that NPs are capable to cause lipid peroxidation of the membrane of *P. tricornutum* (Morelli et al., 2013; Scebba et al., 2016; Deng et al., 2017). Moreover, an increase in the lipid synthesis is in line with the HAADF-STEM analysis showing a great number of lipid vesicles in the cytosol of diatoms cultured with NP12.

The up-regulation of the small ubiquitin-like modifier (SUMO) and a metallopeptidase confirms cell disturbances provoked by NP12 such as genome and protein damage. SUMO is a crucial regulator of signalling proteins in eukaryotes. SUMOylation (protein modification with SUMO) modulates the activity of transcription factors involved in various stress responses in plants, including strong oxidative stress (Bossis and Melchior, 2006). SUMOylation have recently emerged as an important regulatory means to coordinate DNA damage signalling and repair (Pellegrino and Altmeyer, 2016). The up-regulation of a metallopeptidase probably allowed algae cells to remove proteins damaged by NPs and metal ions. They must then be replaced with new copies produced through de novo synthesis. This result is in accordance with a previous study highlighting that NPs and metal ions can impair proteins (oxidation, misfolding) (Pena et al., 2007; Feng et al., 2015; Mirzajani et al., 2014). Moreover, since metallopeptidase are metal-dependent peptidases, cadmium released from NPs could inhibit their function by replacing their essential metal ion. Algae cells must then synthetize a large amount of these enzymes to maintain a vital proteolytic activity. Several previous studies have put forward cadmium–zinc exchanges in proteins (for a review see Tang et al., 2014).

The down-regulation of the TRD3 (Tryptophan Rich Domain) with NP5 and NP12 demonstrates that *P. tricornutum* limited protein damage by decreasing the level of amino-acids which can undergo irreversible oxidative damage. Indeed, a previous study has shown an irreversible ring cleavage of tryptophan under oxidative conditions (Sies, 1986).

In our study, the down-regulation of nucleotide, nucleic acid and RNA binding proteins suggests that CdSe NPs led to a slowdown of the cell division and growth (confirmed by growth kinetics presented in Fig. 2). In contrast, the over-synthesis of numerous structural constituents of ribosomes indicates that *P. tricornutum* greatly increased protein and enzyme synthesis, probably to combat effectively cell disturbances induced by NPs.

Proteomic analysis highlighted the down-regulation of a protein having an adenylate kinase activity in diatoms cultured with NP5. Adenylate kinase, which catalyses the reversible transformation of ADP to ATP and AMP, is a signal transducing protein that regulates cellular energy homeostasis balancing between different conformations (Formoso et al., 2015). Under oxidative stress, it plays a key role to regulate the energy budget, particularly in situations where oxidative phosphorylation is ineffective (Han et al., 2013). In our study, the up-regulation of numerous enzymes involved in oxidation-reduction process could be explained the down-regulation of this enzyme.

Although proteomic analysis has provided some information about defence strategies developed by *P. tricornutum* to counteract CdSe NP toxicity, they did not give us an adequate understanding of mechanisms used by algae cells to decrease the amount of Cd immobilized by cells between the 1- and 4-day incubation times. The up-regulation of a protein involved in the intracellular transport and an integral component of membrane with ATPase activity could be consistent with the hypothesis of an active Cd export as it was also suggested in a previous study (Brembu et al., 2011).

Our study allowed to identify several metabolic changes developed by *P. tricornutum* cells when they are submitted to CdSe NPs. As presented in Fig. 6, the differentially expressed proteins were chiefly involved in the fight against oxidative stress and the cellular redox homeostasis, including Ca^{2+} regulation and signalling, and S-nitrosylation and S-glutathionylation processes. Other regulated proteins were involved in translation; membrane, genomic and protein repair; membrane biogenesis and cell death programming (Fig. 6). Similar responses were also observed when *Oriza sativa* L. was submitted to silver nanoparticles (Mirzajani et al., 2014).

In a previous study, when *P. tricornutum* was cultured with 123 µg/L Cd, the very few transcripts affected indicated that the cells were capable to respond to the increased Cd^{2+} levels without changing proteins levels (Brembu et al., 2011). Thus, the numerous proteome changes observed in our study when *P. tricornutum* was exposed to 2.2×10^{14}

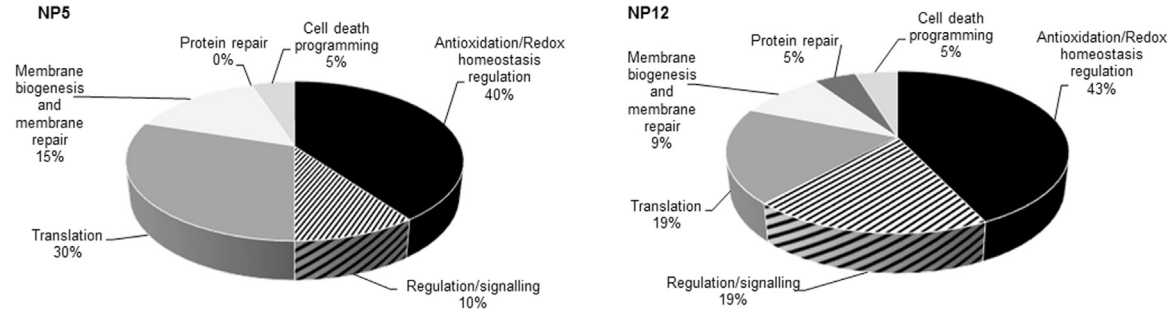

Fig. 6. Distribution of proteins differentially expressed by NP5 (2.2×10^{14} NPs/L, $[Cd]_{eq.}$ = 47 µg/L, $[Se]_{eq.}$ = 33 µg/L) and by NP12 (4.2×10^{13} NPs/L, $[Cd]_{eq.}$ = 127 µg/L, $[Se]_{eq.}$ = 89 µg/L), based on their biological function.

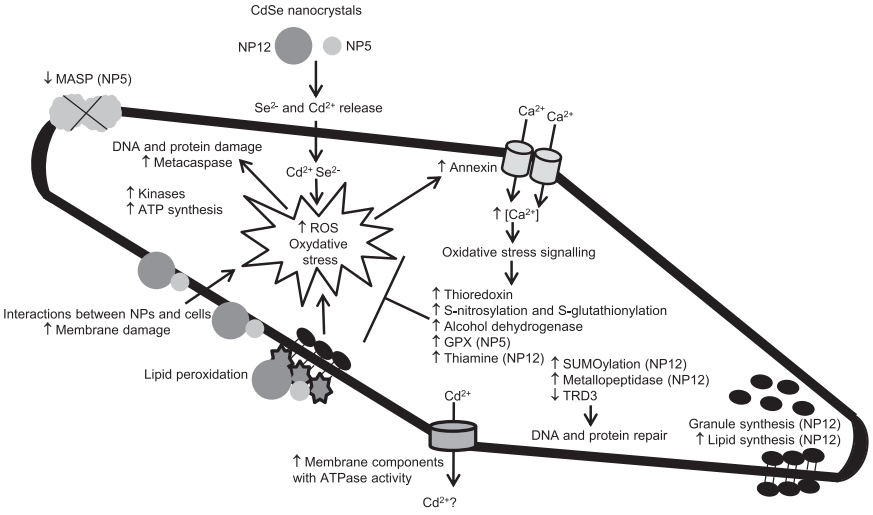

Fig. 7. Schematic representation of a major impact of CdSe NPs on *P. tricornutum*. NP5 (small light grey circles) and NP12 (big dark grey circles) probably interact with algae cells causing membrane damages such as lipid peroxidation. In f/2 medium, the rapid CdSe NP dissolution lead to the release of Cd^{2+} and Se^{2-}, which can enter the cell easily. These two processes induce a ROS generating and a high oxidative stress leading to DNA and protein damage. *P. tricornutum* responded to CdSe NP toxicity by regulating numerous proteins involved in the following defence mechanisms: 1) an effective combat against oxidative stress, and the regulation of cellular redox homeostasis, thanks to annexin, Ca^{2+} regulation and signalling, thioredoxin, S-nitrosylation and S-glutathionylation processes, alcohol dehydrogenase, glutathione peroxidase (GPX), thiamine; 2) a decrease in molecules that can be damaged by NPs and metal ions, e.g., tryptophane rich domain (TRD); 3) a decrease in membrane component promoting NP biosorption, e.g., mucin-associated surface protein (MASP); 4) an increase in regulators and factors involved in stress signalling and DNA damage, e.g., small ubiquitin-like modifier (SUMO), kinase; 5) an increase in synthesis of cell components damaged and inhibited by NPs and metal ions, e.g., lipids and metallopeptidases; 6) a potential active Cd^{+2} export thanks to the up-regulation of an integral component of membrane with ATPse activity; 7) the programmed cell death (PCD) triggers thanks to metacaspase, probably when the ROS generating gets out of control.

NP5/L and 4.2×10^{13} NP12/L, corresponding to 47 µg/L $[Cd]_{eq.}$ and 127 µg/L $[Cd]_{eq.}$, respectively, allow to say that CdSe nanocrystals are more toxic than cadmium ions used at the same concentrations. This is in accordance with previous studies showing that TiO_2 NPs were more harmful than $TiCl_4$ used at the same low Ti concentrations (Minetto et al., 2017) and that ZnO NPs were more toxic than Zn^{2+} (Li et al., 2017). Nevertheless, in our experimental conditions, *P. tricornutum* was capable to counteract CdSe NP toxicity by using major defence mechanisms presented in Fig. 7, but with a decrease in the specific growth rate.

4. Conclusions

Our study confirms that CdSe NPs induce negative impacts on diatoms such as a slow growth, an increase in ROS level and wall damage. The species *P. tricornutum* is more impacted by CdSe NPs than by Cd ions for equivalent Cd concentrations. The high CdSe NP toxicity may be due to direct interactions between CdSe NPs and diatoms, and to the high CdSe dissolution in seawater (100% after 7 days of culture) causing the accumulation of Cd and Se ions inside diatoms. Our study is the first one to use a mass spectrometry-based proteomic approach to identify proteins differentially expressed by *P. tricornutum* subjected to CdSe NPs. The identification of these proteins is fundamental to improve our knowledge about defence mechanisms developed by algae cells to counteract damage caused by CdSe NPs. Proteomic analysis highlighted that *P. tricornutum* responded to CdSe NP toxicity by regulating numerous proteins involved in protection against oxidative stress, cellular redox homeostasis, Ca^{2+} regulation and signalling, S-nitrosylation and S-glutathionylation processes and cell damage repair. These proteome changes allowed diatoms to counteract oxidative stress generated by CdSe NPs and to maintain their growth. Nevertheless, the uptake of CdSe NPs led to the trigger of the programmed cell death and affected the cell concentration.

These findings are relevant because they provide essential information on interactions between diatoms and NPs and help to evaluate the ecological impact of these new pollutants on the marine ecosystems.

Acknowledgements

The authors warmly thank Charlotte Paillet and Claire Guégan for their technical assistance.

This work was financially supported by the “Syndicat Mixte du Cotentin" (AVAL 2013/397 - Des nanoparticules dans l'océan), the "Conseil départemental de la Manche" (CP2017-05-22.4-01-9842) ” and the "Conseil Régional de Basse-Normandie" (Convention 2013 PCM 10 - NANOCEAN).

Appendix A. Supplementary material

Supplementary data associated with this article can be found in the online version at http://dx.doi.org/10.1016/j.ecoenv.2018.01.043.

References

Amini, S., Maali-Amiri, R., Mohammadi, R., Kazemi- Shahandashti, S.-S., 2017. cDNA-AFLP analysis of transcripts induced in chickpea plants by TiO2 nanoparticles during cold stress. Plant Physiol. Biochem. 111, 39–49. http://dx.doi.org/10.1016/j.plaphy.2016.11.011.

Anderson, P., Kedersha, N., 2009. Stress granules. Curr. Biol. 19, R397–R398. http://dx.doi.org/10.1016/j.cub.2009.03.013.

Baker, T.J., Tyler, C.R., Galloway, T.S., 2014. Impacts of metal and metal oxide nanoparticles on marine organisms. Environ. Pollut. 186, 257–271. http://dx.doi.org/10.1016/j.envpol.2013.11.014.

Bathige, S.D.N.K., Umasuthan, N., Godahewa, G.I., Thulasitha, W.S., Whang, I., Won, S.H., Kim, C., Lee, J., 2015. Two variants of selenium-dependent glutathione peroxidase from the disk abalone *Haliotis discus discus*: molecular characterization and immune responses to bacterial and viral stresses. Fish Shellfish Immunol. 45, 648–655. http://dx.doi.org/10.1016/j.fsi.2015.05.028.

Bidle, K.D., 2016. Programmed cell death in unicellular phytoplankton. Curr. Biol. 26, R594–R607. http://dx.doi.org/10.1016/j.cub.2016.05.056.

Bossis, G., Melchior, F., 2006. Regulation of SUMOylation by reversible oxidation of SUMO conjugating enzymes. Mol. Cell 21, 349–357. http://dx.doi.org/10.1016/j.molcel.2005.12.019.

Bowler, C., Allen, A.E., Badger, J.H., Grimwood, J., Jabbari, K., Kuo, A., Maheswari, U., Martens, C., Maumus, F., Otillar, R.P., et al., 2008. The *Phaeodactylum* genome reveals the dynamic nature and multi-lineage evolutionary history of diatom genomes. Nature 456 (7219), 239–244. http://dx.doi.org/10.1038/nature07410.

Brembu, T., Jørstad, M., Winge, P., Valle, K.C., Bones, A.M., 2011. Genome-wide profiling of responses to cadmium in the diatom *Phaeodactylum tricornutum*. Environ. Sci. Technol. 45, 7640–7647. http://dx.doi.org/10.1021/es2002259.

Bukhari, S.A.H., Zheng, W., Xie, L., Zhang, G., Shang, S., Wu, F., 2016. Cr-induced changes in leaf protein profile, ultrastructure and photosynthetic traits in the two contrasting tobacco genotypes. Plant Growth Regul. 79, 147–156. http://dx.doi.org/10.1007/s10725-015-0120-4.

Cabello-Hurtado, F., Lozano-Baena, M.D., Neaime, C., Burel, A., Jeanne, S., Pellen-Mussi, P., Cordier, S., Grasset, F., 2016. Studies on plant cell toxicity of luminescent silica nanoparticles (Cs2[Mo6Br14]@SiO2) and its constitutive components. J. Nanopart. Res. 18. http://dx.doi.org/10.1007/s11051-016-3381-6.

Castro-Bugallo, A., González-Fernández, Á., Guisande, C., Barreiro, A., 2014. Comparative responses to metal oxide nanoparticles in marine phytoplankton. Arch. Environ. Contam. Toxicol. 67, 483–493. http://dx.doi.org/10.1007/s00244-014-0044-4.

Chatziargyriou, V., Dailianis, S., 2010. The role of selenium-dependent glutathione peroxidase (Se-GPx) against oxidative and genotoxic effects of mercury in haemocytes of mussel *Mytilus galloprovincialis* (Lmk.). Toxicol. Vitr. 24, 1363–1372. http://dx.doi.org/10.1016/j.tiv.2010.04.008.

Da Costa, C.H., Perreault, F., Oukarroum, A., Melegari, S.P., Popovic, R., Matias, W.G.,

2016. Effect of chromium oxide (III) nanoparticles on the production of reactive oxygen species and photosystem II activity in the green alga *Chlamydomonas reinhardtii*. Sci. Total Environ. 565, 951–960. http://dx.doi.org/10.1016/j.scitotenv.2016.01.028.

Dailianis, S., Patetsini, E., Kaloyianni, M., 2009. The role of signalling molecules on actin glutathionylation and protein carbonylation induced by cadmium in haemocytes of mussel *Mytilus galloprovincialis* (Lmk). J. Exp. Biol. 212, 3612–3620. http://dx.doi.org/10.1242/jeb.030817.

Deng, Z.J., Mortimer, G., Schiller, T., Musumeci, A., Martin, D., Minchin, R.F., 2009. Differential plasma protein binding to metal oxide nanoparticles. Nanotechnology 20, 455101. http://dx.doi.org/10.1088/0957-4484/20/45/455101.

Deng, X.-Y., Cheng, J., Hu, X.-L., Wang, L., Li, D., Gao, K., 2017. Biological effects of TiO_2 and CeO_2 nanoparticles on the growth, photosynthetic activity, and cellular components of a marine diatom *Phaeodactylum tricornutum*. Sci. Total Environ. 575, 87–96. http://dx.doi.org/10.1016/j.scitotenv.2016.10.003.

Derfus, A.M., Chan, W.C.W., Bhatia, S.N., 2004. Probing the cytotoxicity of semiconductor quantum dots. Nano Lett. 4, 11–18. http://dx.doi.org/10.1021/nl0347334.

Elsayed, K.N.M., Kolesmikova, T.A., Noke, A., Klöck, G., 2017. Imaging the accumulated intracellular microalgal lipids as a response to temperature stress. 3 Biotech 7, 41. http://dx.doi.org/10.1007/s13205-017-0677-x.

Fagundes, D., Bohn, B., Cabreira, C., Leipelt, F., Dias, N., Bodanese-Zanettini, M.H., Cagliari, A., 2015. Caspases in plants: metacaspase gene family in plant stress responses. Funct. Integr. Genom. 15, 639–649. http://dx.doi.org/10.1007/s10142-015-0459-7.

Feng, P.-H., Huang, Y.-L., Chuang, K.-J., Chen, K.-Y., Lee, K.-Y., Ho, S.-C., Bien, M.-Y., Yang, Y.-L., Chuang, H.-C., 2015. Dysfunction of methionine sulfoxide reductases to repair damaged proteins by nickel nanoparticles. Chem.-Biol. Interact. 236, 82–89. http://dx.doi.org/10.1016/j.cbi.2015.05.003.

Formoso, E., Limongelli, V., Parrinello, M., 2015. Energetics and structural characterization of the large-scale functional motion of adenylate kinase. Sci. Rep. 5. http://dx.doi.org/10.1038/srep08425.

Go, Y.-M., Orr, M., Jones, D.P., 2013. Actin cytoskeleton redox proteome oxidation by cadmium. AJP: Lung Cell. Mol. Physiol. 305, L831–L843. http://dx.doi.org/10.1152/ajplung.00203.2013.

Gojkovic, Ž., Garbayo, I., Ariza, J.L.G., Márová, I., Vílchez, C., 2015. Selenium bioaccumulation and toxicity in cultures of green microalgae. Algal Res. 7, 106–116. http://dx.doi.org/10.1016/j.algal.2014.12.008.

González-Pleiter, M., Rioboo, C., Reguera, M., Abreu, I., Leganés, F., Cid, Á., Fernández-Piñas, F., 2017. Calcium mediates the cellular response of *Chlamydomonas reinhardtii* to the emerging aquatic pollutant Triclosan. Aquat. Toxicol. 186, 50–66. http://dx.doi.org/10.1016/j.aquatox.2017.02.021.

Gottschalk, F., Sun, T., Nowack, B., 2013. Environmental concentrations of engineered nanomaterials: review of modeling and analytical studies. Environ. Pollut. 181, 287–300. http://dx.doi.org/10.1016/j.envpol.2013.06.003.

Han, G.-d., Zhang, S., Marshall, D.J., Ke, C.-h., Dong, Y.-w., 2013. Metabolic energy sensors (AMPK and SIRT1), protein carbonylation and cardiac failure as biomarkers of thermal stress in an intertidal limpet: linking energetic allocation with environmental temperature during aerial emersion. J. Exp. Biol. 216, 3273–3282. http://dx.doi.org/10.1242/jeb.084269.

Hetsch, F., Xu, X., Wang, H., Kershaw, S.V., Rogach, A.L., 2011. Semiconductor nanocrystal quantum dots as solar cell components and photosensitizers: material, charge transfer, and separation aspects of some device topologies. J. Phys. Chem. Lett. 2, 1879–1887. http://dx.doi.org/10.1021/jz200802j.

Jiang, Y., Zhu, Y., Hu, Z., Lei, A., Wang, J., 2016. Towards elucidation of the toxic mechanism of copper on the model green alga *Chlamydomonas reinhardtii*. Ecotoxicology 25, 1417–1425. http://dx.doi.org/10.1007/s10646-016-1692-0.

Jung, I.L., Kim, I.G., 2003. Thiamine protects against paraquat-induced damage: scavenging activity of reactive oxygen species. Environ. Toxicol. Pharmacol. 15, 19–26. http://dx.doi.org/10.1016/j.etap.2003.08.001.

Khan, M.I.R., Nazir, F., Asgher, M., Per, T.S., Khan, N.A., 2015. Selenium and sulfur influence ethylene formation and alleviate cadmium-induced oxidative stress by improving proline and glutathione production in wheat. J. Plant Physiol. 173, 9–18. http://dx.doi.org/10.1016/j.jplph.2014.09.011.

Kim, M.-J., Lee, B.C., Hwang, K.Y., Gladyshev, V.N., Kim, H.-Y., 2015. Selenium utilization in thioredoxin and catalytic advantage provided by selenocysteine. Biochem. Biophys. Res. Commun. 461, 648–652. http://dx.doi.org/10.1016/j.bbrc.2015.04.082.

Kirchner, C., Liedl, T., Kudera, S., Pellegrino, T., Muñoz Javier, A., Gaub, H.E., Stölzle, S., Fertig, N., Parak, W.J., 2005. Cytotoxicity of colloidal CdSe and CdSe/ZnS nanoparticles. Nano Lett. 5, 331–338. http://dx.doi.org/10.1021/nl047996m.

Laohavisit, A., Brown, A.T., Cicuta, P., Davies, J.M., 2010. Annexins: components of the calcium and reactive oxygen signaling network. Plant Physiol. 152, 1824–1829. http://dx.doi.org/10.1104/pp.109.145458.

Le Costaouëc, T., Unamunzaga, C., Mantecon, L., Helbert, W., 2017. New structural insights into the cell-wall polysaccharide of the diatom *Phaeodactylum tricornutum*. Algal Res. 26, 172–179. http://dx.doi.org/10.1016/j.algal.2017.07.021.

Li, J., Schiavo, S., Rametta, G., Miglietta, M.L., La Ferrara, V., Wu, C., Manzo, S., 2017. Comparative toxicity of nano ZnO and bulk ZnO towards marine algae *Tetraselmis suecica* and *Phaeodactylum tricornutum*. Environ. Sci. Pollut. Res. 24, 6543–6553. http://dx.doi.org/10.1007/s11356-016-8343-0.

Lin, S., Bhattacharya, P., Rajapakse, N.C., Brune, D.E., Ke, P.C., 2009. Effects of quantum dots adsorption on algal photosynthesis. J. Phys. Chem. C 113, 10962–10966. http://dx.doi.org/10.1021/jp904343s.

Lu, J., Holmgren, A., 2014. The thioredoxin antioxidant system. Free Radic. Biol. Med. 66, 75–87. http://dx.doi.org/10.1016/j.freeradbiomed.2013.07.036.

Macfie, S.M., Welbourn, P.M., 2000. The cell wall as a barrier to uptake of metal ions in the unicellular green alga *Chlamydomonas reinhardtii* (Chlorophyceae). Arch. Environ. Contam. Toxicol. 39, 413–419. http://dx.doi.org/10.1007/s002440010122.

Marchand, C., Le Maréchal, P., Meyer, Y., Decottignies, P., 2006. Comparative proteomic approaches for the isolation of proteins interacting with thioredoxin. Proteomics 6, 6528–6537. http://dx.doi.org/10.1002/pmic.200600443.

Martínez-Ruiz, E.B., Martínez-Jerónimo, F., 2015. Nickel has biochemical, physiological, and structural effects on the green microalga *Ankistrodesmus falcatus*: an integrative study. Aquat. Toxicol. 169, 27–36. http://dx.doi.org/10.1016/j.aquatox.2015.10.007.

Minetto, D., Libralato, G., Marcomini, A., Volpi Ghirardini, A., 2017. Potential effects of TiO2 nanoparticles and TiCl4 in saltwater to *Phaeodactylum tricornutum* and *Artemia franciscana*. Sci. Total Environ. 579, 1379–1386. http://dx.doi.org/10.1016/j.scitotenv.2016.11.135.

Mirzajani, F., Askari, H., Hamzelou, S., Schober, Y., Römpp, A., Ghassempour, A., Spengler, B., 2014. Proteomics study of silver nanoparticles toxicity on *Oryza sativa* L. Ecotoxicol. Environ. Saf. 108, 335–339. http://dx.doi.org/10.1016/j.ecoenv.2014.07.013.

Monrás, J.P., Collao, B., Molina-Quiroz, R.C., Pradenas, G.A., Saona, L.A., Durán-Toro, V., Órdenes-Aenishanslins, N., Venegas, F.A., Loyola, D.E., Bravo, D., et al., 2014. Microarray analysis of the *Escherichia coli* response to CdTe-GSH quantum dots: understanding the bacterial toxicity of semiconductor nanoparticles. BMC Genom. 15, 1099. http://dx.doi.org/10.1186/1471-2164-15-1099.

Morelli, E., Cioni, P., Posarelli, M., Gabellieri, E., 2012. Chemical stability of CdSe quantum dots in seawater and their effects on a marine microalga. Aquat. Toxicol. 122–123, 153–162. http://dx.doi.org/10.1016/j.aquatox.2012.06.012.

Morelli, E., Salvadori, E., Bizzarri, R., Cioni, P., Gabellieri, E., 2013. Interaction of CdSe/ZnS quantum dots with the marine diatom *Phaeodactylum tricornutum* and the green alga *Dunaliella tertiolecta*: a biophysical approach. Biophys. Chem. 182, 4–10. http://dx.doi.org/10.1016/j.bpc.2013.06.007.

Morelli, E., Salvadori, E., Basso, B., Tognotti, D., Cioni, P., Gabellieri, E., 2015. The response of *Phaeodactylum tricornutum* to quantum dot exposure: acclimation and changes in protein expression. Mar. Environ. Res. 111, 149–157. http://dx.doi.org/10.1016/j.marenvres.2015.06.018.

Morones, J.R., Elechiguerra, J.L., Camacho, A., Holt, K., Kouri, J.B., Ramírez, J.T., Yacaman, M.J., 2005. The bactericidal effect of silver nanoparticles. Nanotechnology 16, 2346–2353. http://dx.doi.org/10.1088/0957-4484/16/10/059.

Pellegrino, S., Altmeyer, M., 2016. Interplay between ubiquitin, SUMO, and Poly(ADP-Ribose) in the cellular response to genotoxic Stress. Front. Genet. 7. http://dx.doi.org/10.3389/fgene.2016.00063.

Pena, L.B., Pasquini, L.A., Tomaro, M.L., Gallego, S.M., 2007. 20S proteasome and accumulation of oxidized and ubiquitinated proteins in maize leaves subjected to cadmium stress. Phytochemistry 68, 1139–1146. http://dx.doi.org/10.1016/j.phytochem.2007.02.022.

Peng, C., Zhang, W., Gao, H., Li, Y., Tong, X., Li, K., Zhu, X., Wang, Y., Chen, Y., 2017. Behavior and potential impacts of metal-based engineered nanoparticles in aquatic environments. Nanomaterials 7, 21. http://dx.doi.org/10.3390/nano7010021.

Pittman, J.K., 2011. Vacuolar Ca^{2+} uptake. Cell Calcium 50, 139–146. http://dx.doi.org/10.1016/j.ceca.2011.01.004.

Poirier, I., Jean, N., Guary, J.C., Bertrand, M., 2008. Responses of the marine bacterium *Pseudomonas fluorescens* to an excess of heavy metals: physiological and biochemical aspects. Sci. Total Environ. 406, 76–87. http://dx.doi.org/10.1016/j.scitotenv.2008.07.038.

Poirier, I., Kuhn, L., Caplat, C., Hammann, P., Bertrand, M., 2014. The effect of cold stress on the proteome of the marine bacterium *Pseudomonas fluorescens* BA3SM1 and its ability to cope with metal excess. Aquat. Toxicol. 157, 120–133. http://dx.doi.org/10.1016/j.aquatox.2014.10.002.

Poirier, I., Kuhn, L., Demortière, A., Mirvaux, B., Hammann, P., Chicher, J., Caplat, C., Pallud, M., Bertrand, M., 2016. Ability of the marine bacterium *Pseudomonas fluorescens* BA3SM1 to counteract the toxicity of CdSe nanoparticles. J. Proteom. 148, 213–227. http://dx.doi.org/10.1016/j.jprot.2016.07.021.

Qian, H., Zhu, K., Lu, H., Lavoie, M., Chen, S., Zhou, Z., Deng, Z., Chen, J., Fu, Z., 2016. Contrasting silver nanoparticle toxicity and detoxification strategies in *Microcystis aeruginosa* and *Chlorella vulgaris*: new insights from proteomic and physiological analyses. Sci. Total Environ. 572, 1213–1221. http://dx.doi.org/10.1016/j.scitotenv.2016.08.039.

Raize, O., Argaman, Y., Yannai, S., 2004. Mechanisms of biosorption of different heavy metals by brown marine macroalgae. Biotechnol. Bioeng. 87, 451–458. http://dx.doi.org/10.1002/bit.20136.

Rocha, T.L., Mestre, N.C., Sabóia-Morais, S.M.T., Bebianno, M.J., 2017. Environmental behaviour and ecotoxicity of quantum dots at various trophic levels: a review. Environ. Int. 98, 1–17. http://dx.doi.org/10.1016/j.envint.2016.09.021.

Rzigalinski, B.A., Strobl, J.S., 2009. Cadmium-containing nanoparticles: perspectives on pharmacology and toxicology of quantum dots☆. Toxicol. Appl. Pharmacol. 238, 280–288. http://dx.doi.org/10.1016/j.taap.2009.04.010.

Saidi, I., Chtourou, Y., Djebali, W., 2014. Selenium alleviates cadmium toxicity by preventing oxidative stress in sunflower (*Helianthus annuus*) seedlings. J. Plant Physiol. 171, 85–91. http://dx.doi.org/10.1016/j.jplph.2013.09.024.

Santimano, M.C., Martin, A., Kowshik, M., Sarkar, A., 2013. Zinc oxide nanoparticles cause morphological changes in human A549 cell line through alteration in the expression pattern of small GTPases at mRNA level. J. Bionanosci. 7, 300–306. http://dx.doi.org/10.1166/jbns.2013.1134.

Scebba, F., Tognotti, D., Presciuttini, G., Gabellieri, E., Cioni, P., Angeloni, D., Basso, B., Morelli, E., 2016. A SELDI-TOF approach to ecotoxicology: comparative profiling of low molecular weight proteins from a marine diatom exposed to CdSe/ZnS quantum dots. Ecotoxicol. Environ. Saf. 123, 45–52. http://dx.doi.org/10.1016/j.ecoenv.2015.

08.024.
Schiavo, S., Duroudier, N., Bilbao, E., Mikolaczyk, M., Schäfer, J., Cajaraville, M.P., Manzo, S., 2017. Effects of PVP/PEI coated and uncoated silver NPs and PVP/PEI coating agent on three species of marine microalgae. Sci. Total Environ. 577, 45–53. http://dx.doi.org/10.1016/j.scitotenv.2016.10.051.
Sendra, M., Yeste, M.P., Gatica, J.M., Moreno-Garrido, I., Blasco, J., 2017a. Direct and indirect effects of silver nanoparticles on freshwater and marine microalgae (*Chlamydomonas reinhardtii* and *Phaeodactylum tricornutum*). Chemosphere 179, 279–289. http://dx.doi.org/10.1016/j.chemosphere.2017.03.123.
Sendra, M., Yeste, P.M., Moreno-Garrido, I., Gatica, J.M., Blasco, J., 2017b. CeO2 NPs, toxic or protective to phytoplankton? Charge of nanoparticles and cell wall as factors which cause changes in cell complexity. Sci. Total Environ. 590–591, 304–315. http://dx.doi.org/10.1016/j.scitotenv.2017.03.007.
She, C., Demortière, A., Shevchenko, E.V., Pelton, M., 2011. Using shape to control photoluminescence from CdSe/CdS core/shell nanorods. J. Phys. Chem. Lett. 2, 1469–1475. http://dx.doi.org/10.1021/jz200510f.
She, C., Bryant, G.W., Demortière, A., Shevchenko, E.V., Pelton, M., 2013. Controlling the spatial location of photoexcited electrons in semiconductor CdSe/CdS core/shell nanorods. Phys. Rev. B - Condens. Matter Mater. Phys. 87, 155427. http://dx.doi.org/10.1103/PhysRevB.87.155427.
Shebanova, A., Ismagulova, T., Solovchenko, A., Baulina, O., Lobakova, E., Ivanova, A., Moiseenko, A., Shaitan, K., Polshakov, V., Nedbal, L., Gorelova, O., 2017. Versatility of the green microalga cell vacuole function as revealed by analytical transmission electron microscopy. Protoplasma 254, 1323–1340. http://dx.doi.org/10.1007/s00709-016-1024-5.
Shelton, M.D., Chock, P.B., Mieyal, J.J., 2005. Glutaredoxin: role in reversible protein S-glutathionylation and regulation of redox signal transduction and protein translocation. Antioxid. Redox Signal. 7, 348–366. http://dx.doi.org/10.1089/ars.2005.7.348.
Sies, H., 1986. Biochemistry of oxidative stress. Angew. Chem. Int. Ed. Engl. 5, 1058–1071. http://dx.doi.org/10.1042/BST0351147.
Stark, W.J., Stoessel, P.R., Wohlleben, W., Hafner, A., 2015. Industrial applications of nanoparticles. Chem. Soc. Rev. 44, 5793–5805. http://dx.doi.org/10.1039/c4cs00362d.
Sylvander, P., Häubner, N., Snoeijs, P., 2013. The thiamine content of phytoplankton cells is affected by abiotic stress and growth rate. Microb. Ecol. 65, 566–577. http://dx.doi.org/10.1007/s00248-012-0156-1.
Tang, L., Qiu, R., Tang, Y., Wang, S., 2014. Cadmium-zinc exchange and their binary relationship in the structure of Zn-related proteins: a mini review. Metallomics 6, 1313–1323. http://dx.doi.org/10.1039/c4mt00080c.
Tang, Y., Li, S., Lu, Y., Li, Q., Yu, S., 2015. The influence of humic acid on the toxicity of nano-ZnO and Zn^{2+} to the *Anabaena* sp. Environ. Toxicol. 30, 895–903. http://dx.doi.org/10.1002/tox.21964.
Torres, E., Cid, A., Herrero, C., Abalde, J., 2000. Effect of cadmium on growth, ATP content, carbon fixation and ultrastructure in the marine diatom *Phaeodactylum tricornutum* Bohlin. Water, Air, Soil Pollut. 117, 1–14. http://dx.doi.org/10.1023/A:1005121012697.
Torres, E., Mera, R., Herrero, C., Abalde, J., 2014. Isotherm studies for the determination of Cd (II) ions removal capacity in living biomass of a microalga with high tolerance to cadmium toxicity. Environ. Sci. Pollut. Res. 21, 12616–12628. http://dx.doi.org/10.1007/s11356-014-3207-y.
Tunc-Ozdemir, M., Miller, G., Song, L., Kim, J., Sodek, A., Koussevitzky, S., Misra, A.N., Mittler, R., Shintani, D., 2009. Thiamin confers enhanced tolerance to oxidative stress in *Arabidopsis*. Plant Physiol. 151, 421–432. http://dx.doi.org/10.1104/pp.109.140046.
Van Hoewyk, D., Takahashi, H., Inoue, E., Hess, A., Tamaoki, M., Pilon-Smits, E.A.H., 2008. Transcriptome analyses give insights into selenium-stress responses and selenium tolerance mechanisms in *Arabidopsis*. Physiol. Plant. 132, 236–253. http://dx.doi.org/10.1111/j.1399-3054.2007.01002.x.
Vatansever, R., Filiz, E., Ozyigit, I.I., 2016. In silico analysis of Mn transporters (NRAMP1) in various plant species. Mol. Biol. Rep. 43, 151–163. http://dx.doi.org/10.1007/s11033-016-3950-x.
Vercruysse, M., Fauvart, M., Jans, A., Beullens, S., Braeken, K., Cloots, L., Engelen, K., Marchal, K., Michiels, J., 2011. Stress response regulators identified through genome-wide transcriptome analysis of the (p) ppGpp-dependent response in *Rhizobium etli*. Genome Biol. 12, R17. http://dx.doi.org/10.1186/gb-2011-12-2-r17.
Verdin, A., Lounès-Hadj Sahraoui, A., Newsam, R., Robinson, G., Durand, R., 2005. Polycyclic aromatic hydrocarbons storage by *Fusarium solani* in intracellular lipid vesicles. Environ. Pollut. 133, 283–291. http://dx.doi.org/10.1016/j.envpol.2004.05.040.
Vidal, R., Lopez-Maury, L., Guerrero, M.G., Florencio, F.J., 2009. Characterization of an alcohol dehydrogenase from the cyanobacterium *Synechocystis* sp. Strain PCC 6803 that responds to environmental stress conditions via the Hik34-Rre1 two-component system. J. Bacteriol. 191, 4383–4391. http://dx.doi.org/10.1128/JB.00183-09.
Walsh, G.E., 1993. Primary producers. In: Calow, P. (Ed.), Handbook of Ecotoxicology 1. Blackwell Scientific, Oxford, UK, pp. 119–144. http://dx.doi.org/10.1002/9781444313512.ch8.
Wang, H., Joseph, J.A., 1999. Quantifying cellular oxidative stress by dichlorofluorescein assay using microplate reader. Free Radic. Biol. Med. 27, 612–616. http://dx.doi.org/10.1016/S0891-5849(99)00107-0.
Wang, Y., Zhu, X., Lao, Y., Lv, X., Tao, Y., Huang, B., Wang, J., Zhou, J., Cai, Z., 2016. TiO2 nanoparticles in the marine environment: physical effects responsible for the toxicity on algae *Phaeodactylum tricornutum*. Sci. Total Environ. 565, 818–826. http://dx.doi.org/10.1016/j.scitotenv.2016.03.164.
Wang, H., Mi, T., Zhen, Y., Jing, X., Liu, Q., Yu, Z., 2017. Metacaspases and programmed cell death in *Skeletonema marinoi* in response to silicate limitation. J. Plankton Res. 39, 729–743. http://dx.doi.org/10.1093/plankt/fbw090.
Wolak, N., Kowalska, E., Kozik, A., Rapala-Kozik, M., 2014. Thiamine increases the resistance of baker's yeast *Saccharomyces cerevisiae* against oxidative, osmotic and thermal stress, through mechanisms partly independent of thiamine diphosphate-bound enzymes. FEMS Yeast Res. 14, 1249–1262. http://dx.doi.org/10.1111/1567-1364.12218.
Wong, K.V., Perilla, N., Paddon, A., 2014. Nanoscience and nanotechnology in solar cells. J. Energy Resour. Technol. 136, 014001. http://dx.doi.org/10.1115/1.4024715.
Xia, B., Chen, B., Sun, X., Qu, K., Ma, F., Du, M., 2015. Interaction of TiO_2 nanoparticles with the marine microalga *Nitzschia closterium:* Growth inhibition, oxidative stress and internalization. Sci. Total Environ. 508, 525–533. http://dx.doi.org/10.1016/j.scitotenv.2014.11.066.
Zeng, C., Ramos-Ruiz, A., Field, J.A., Sierra-Alvarez, R., 2015. Cadmium telluride (CdTe) and cadmium selenide (CdSe) leaching behavior and surface chemistry in response to pH and O_2. J. Environ. Manag. 154, 78–85. http://dx.doi.org/10.1016/j.jenvman.2015.02.033.
Zhang, X., Tang, X., Wang, M., Zhang, W., Zhou, B., Wang, Y., 2017. ROS and calcium signaling mediated pathways involved in stress responses of the marine microalgae *Dunaliella salina* to enhanced UV-B radiation. J. Photochem. Photobiol. B: Biol. 173, 360–367. http://dx.doi.org/10.1016/j.jphotobiol.2017.05.038.
Zhou, C., Vitiello, V., Pellegrini, D., Wu, C., Morelli, E., Buttino, I., 2016. Toxicological effects of CdSe/ZnS quantum dots on marine planktonic organisms. Ecotoxicol. Environ. Saf. 123, 26–31. http://dx.doi.org/10.1016/j.ecoenv.2015.09.020.
Zhu, Y., Xu, J., Lu, T., Zhang, M., Ke, M., Fu, Z., Pan, X., Qian, H., 2017. A comparison of the effects of copper nanoparticles and copper sulfate on *Phaeodactylum tricornutum* physiology and transcription. Environ. Toxicol. Pharmacol. 56, 43–49. http://dx.doi.org/10.1016/j.etap.2017.08.029.